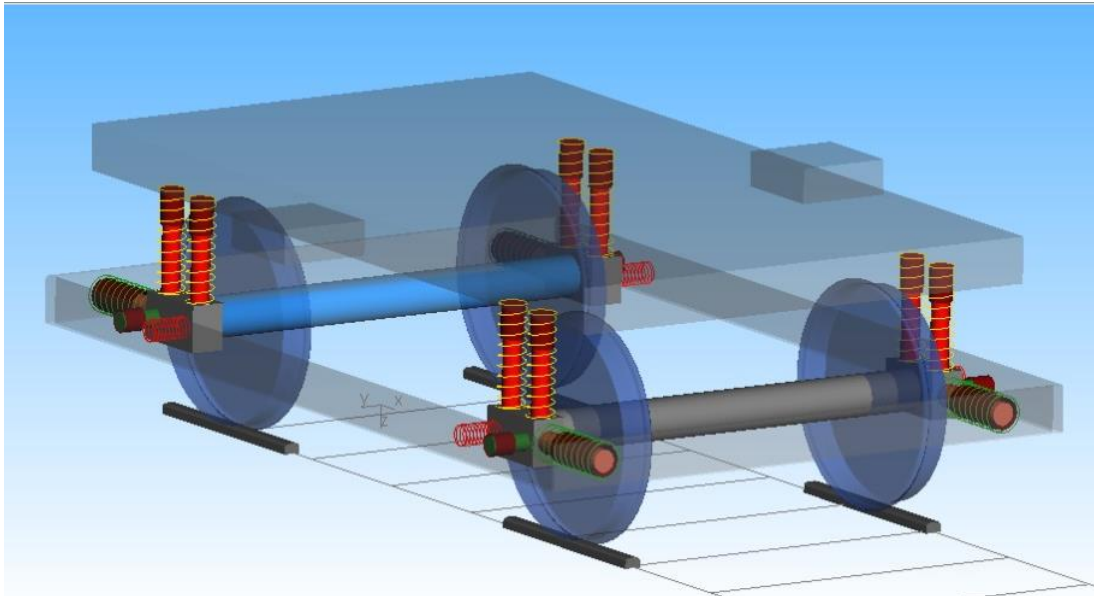


CHALMERS



Towards optimization of a high speed train bogie primary suspension

Master's Thesis in the International Master's programme Applied Mechanics

ADRIÁN HERRERO

Department of Applied Mechanics
Division of Dynamics

CHALMERS UNIVERSITY OF TECHNOLOGY
Göteborg, Sweden 2013
Master's thesis 2013:63

MASTER'S THESIS IN INTERNATIONAL MASTER'S PROGRAMME APPLIED
MECHANICS

Towards optimization of a high speed train bogie primary
suspension

ADRIÁN HERRERO

Department of Applied Mechanics
Division of Dynamics
CHALMERS UNIVERSITY OF TECHNOLOGY
Göteborg, Sweden 2013

Towards optimization of a high speed train bogie primary suspension
ADRIÁN HERRERO

© ADRIÁN HERRERO, 2013

Master's Thesis 2013:63
ISSN 1652-8557

Department of Applied Mechanics
Division of Dynamics
Chalmers University of Technology
SE-412 96 Göteborg
Sweden
Telephone: + 46 (0)31-772 1000

Chalmers Reproservice
Göteborg, Sweden 2013

Towards optimization of a high speed train bogie primary suspension
Master's Thesis in the *International Master's programme Applied Mechanics*

ADRIÁN HERRERO

Department of Applied Mechanics

Division of Dynamics

Chalmers University of Technology

Abstract

Railways provide a safe and fast way of transportation. As a matter of higher speeds demands, railway companies are forced to meet more restrictive and severe specifications concerning the dynamics behaviour of their railway vehicles. One of the main possibilities to achieve this aim is the improvement of the railway vehicle suspensions. This work is focused on the optimization of the primary passive suspension of a high speed train with the aim of improving the dynamics behaviour in terms of ride comfort and wheel-rail wear objective functions, while safety is considered as a threshold. Multi-Body Simulation software SIMPACK rail is employed to create a 50 DOFs one car railway vehicle model with two bogies. To verify the simulation results, the SIMPACK model is run on five operational scenarios (with measured data as the track irregularities) and ride comfort, safety and wear objective functions are evaluated and compared with the admissible values from different railway standards. MATLAB SIMULINK-SIMPACT connection is put into practice with the purpose of running the Genetic Algorithm based optimization routines.

The first set of optimization problems are focused on the optimization of the bogie primary suspension springs and dampers components with respect to the wheel-rail wear objective function while ride comfort and safety are taken as thresholds. The results obtained show a significant reduction in the wear rate while keeping the remaining objective functions within the admissible limits. In addition and using the results from the first set of optimization problems, a pair of bi-objective optimization problems with wheel-rail wear and ride comfort as objective functions are considered through the variation of the bogie primary suspension springs and dampers characteristics as design parameters.

The optimized values of design parameters (bogie primary suspension stiffness and damping) are found for each operational scenario. The optimization results achieved can be used as a guideline to improve the performance of existing bogie primary suspensions and give some hints for design and implementation of semi-active or fully active suspensions.

Key words: Railway vehicle, passive primary suspension, safety, ride comfort, wheel-rail wear, SIMPACK, Matlab/Simulink, co-simulation.

Table of Contents

Abstract	I
Table of Contents	III
Preface.....	V
List of Figures	VI
List of Tables.....	IX
Notations	X
1 Introduction.....	1
1.1 Research background and aims	1
1.2 Literature review	3
1.3 Purpose of the project.....	5
2 Objective Functions	6
2.1 Ride comfort.....	6
2.1.1 Wertungszahl (Wz)	6
2.1.2 UNE – ENV 12299	8
2.2 Safety.....	10
2.2.1 Track shift forces.....	10
2.2.2 Derailment coefficient.....	10
2.3 Rail–wheel wear	11
3 SIMPACK modelling	12
3.1 Modelling in SIMPACK v9.4 rail module	12
3.1.1 “Rail - Wheel Pair” panel.....	12
3.1.2 “Track Pair” panel.....	13
3.1.3 “Rail – Wheel Contacts” panel	14
3.1.4 Bodies.....	14
3.1.5 Track definition.....	15
3.1.6 Static equilibrium and preload calculation.....	16
3.1.7 “Solver Settings” panel: time integration off-line and on-line.....	17
3.2 Railway vehicle model created for the simulations.....	18
3.2.1 “Rail – Wheel pair” panel–Railway vehicle model	21
3.2.2 “Track Pair” panel–Railway vehicle model	22
3.2.3 “Rail – Wheel contacts” panel–Railway vehicle model.....	22
3.2.4 Track definition–Railway vehicle model	22
3.2.5 “Solver Settings” panel – Railway vehicle model	23
3.2.6 Railway vehicle model description–Engineering model.....	23

3.2.7	Railway vehicle model suspension strategy: primary and secondary suspension	24
4	Reference model assessment and verification	27
4.1	Operational scenarios for the reference assessment	27
4.1.1	Straight track scenario	27
4.1.2	Curved track scenario	28
4.1.3	Track irregularities	32
4.1.4	Scenarios for reference assessment – Table resume	32
4.2	Reference model assessment-Objective functions evaluation	33
4.2.1	Objective functions limit values	33
4.2.2	Reference model assessment: Objective functions value	34
5	Optimization, results and discussion	36
5.1	MATLAB-SIMPACK connection	36
5.1.1	MATLAB role	36
5.1.2	SIMULINK role	37
5.1.3	SIMAT Block	37
5.1.4	SIMPACK role	38
5.2	Genetic Algorithm method	39
5.3	Rail–wheel wear optimization	40
5.3.1	Wear optimization with longitudinal and lateral primary stiffness as design parameters	40
5.3.2	Wear optimization with respect to the primary damping coefficients ...	45
5.4	Rail–wheel wear and ride comfort optimization	51
5.4.1	Rail–wheel wear and ride comfort optimization with longitudinal and lateral primary stiffness as design parameters	51
5.4.2	Wear and ride comfort optimization with primary dampers as design parameters	58
6	Conclusion	67
6.1	Summary	67
6.2	Future work	68
7	References	69

Preface

The work presented in this thesis is carried out at the Division of Dynamics, Applied Mechanics Department, Chalmers University of Technology (Göteborg, Sweden) as the last step of the course Mechanical Engineering in Mechanical Systems Design taught at Politecnico di Milano University.

I would like to express my gratitude to Professor Giorgio Previati for giving me support on realizing my Master Thesis abroad.

It's my pleasure to declare my profound sense of gratitude to Professor Viktor Berbyuk, my supervisor and examiner at Chalmers, for providing me the opportunity of realizing this project.

I owe a deep sense of affection to Mr. Seyed Milad Mousavi Bideleh, my supervisor at Chalmers, for providing me help and wise advices throughout the development of this work.

This project is dedicated to two very special people, Jara and Ignacio.

List of Figures

Figure 2.1	Frequency weighting functions for W_z [Sperling and Betzhold (1956)].	7
Figure 2.2	Frequency weighting functions for W_{ad} [CEN (1999)].	8
Figure 2.3	Frequency weighting functions for W_{ab} [CEN (1999)].	9
Figure 3.1	“Rail-Wheel Pair” panel.	13
Figure 3.2	“Track Pair” panel.	13
Figure 3.3	“Body properties” panel.	14
Figure 3.4	“Track Properties - Layout” panel	15
Figure 3.5	“Track Properties - Excitation” panel	15
Figure 3.6	Preload calculation menu.	16
Figure 3.7	Static equilibrium menu.	17
Figure 3.8	“Solver Settings” panel.	17
Figure 3.9	Top view of reference railway model [Cheng, Lee, Chen (2009)].	19
Figure 3.10	Front view of reference railway model [Cheng, Lee, Chen (2009)].	19
Figure 3.11	Railway model used during the simulations.	20
Figure 3.12	Bogie frame connected to wheelsets by the primary suspension.	20
Figure 3.13	Detail of the primary suspension.	21
Figure 3.14	Track irregularities in lateral direction.	22
Figure 3.15	Track irregularities in vertical direction.	22
Figure 3.16	Track irregularities in gauge direction.	23
Figure 3.17	Track irregularities in roll direction.	23
Figure 3.18	Primary suspension.	24
Figure 3.19	Secondary suspension.	24
Figure 3.20	Bumpstop force element located between rear bogie and car frame.	25
Figure 3.21	Bumpstop function [x axis (m), y axis (N)].	26
Figure 4.1	Straight track layout representation.	27
Figure 4.2	Track plane acceleration [Anderson, Berg and Stichel (2007)].	28
Figure 4.3	Track characteristics [Anderson, Berg and Stichel (2007)].	28
Figure 4.4	Zone 4 curved track layout representation.	30
Figure 4.5	Zone 3 curved track layout representation.	31
Figure 4.6	Zone 2 curved track layout representation.	31
Figure 4.7	Zone 1 curved track layout representation.	32
Figure 4.8	Track shift forces for reference assessment.	34
Figure 4.9	Derailment coefficient for reference assessment.	34

Figure 4.10	Ride comfort for reference assessment.....	35
Figure 4.11	Wear number for reference assessment.	35
Figure 5.1	SIMULINK – SIMPACK connection by the use of the SIMAT block.	37
Figure 5.2	SIMAT block in a SIMULINK file.....	37
Figure 5.3	SIMAT block interface.	38
Figure 5.4	Results from $\Gamma_{WEAR}(k_X, k_Y)$ optimization in every scenario.	41
Figure 5.5	Longitudinal primary stiffness value in $\Gamma_{WEAR}(k_X, k_Y)$	42
Figure 5.6	Lateral primary stiffness value in $\Gamma_{WEAR}(k_X, k_Y)$	42
Figure 5.7	Track shift force values in $\Gamma_{WEAR}(k_X, k_Y)$	43
Figure 5.8	Derailment coefficient values in $\Gamma_{WEAR}(k_X, k_Y)$	44
Figure 5.9	Results from $\Gamma_{WEAR}(c^P_X, c^P_Y, c^P_Z)$ optimization in every scenario.	46
Figure 5.10	Longitudinal primary damping coefficient value in $\Gamma_{WEAR}(c^P_X, c^P_Y, c^P_Z)$. 47	47
Figure 5.11	Lateral primary damping coefficient value in $\Gamma_{WEAR}(c^P_X, c^P_Y, c^P_Z)$. ..	48
Figure 5.12	Vertical primary damping coefficient value in $\Gamma_{WEAR}(c^P_X, c^P_Y, c^P_Z)$..	49
Figure 5.13	Track shift force values in $\Gamma_{WEAR}(c^P_X, c^P_Y, c^P_Z)$	49
Figure 5.14	Derailment coefficient values in $\Gamma_{WEAR}(c^P_X, c^P_Y, c^P_Z)$	50
Figure 5.15	Pareto-front for Zone4 scenario in $F(k_X, k_Y)$ problem.....	52
Figure 5.16	Pareto-sets for Zone4 scenario in $F(k_X, k_Y)$ problem.	53
Figure 5.17	Pareto-front for Zone3 scenario in $F(k_X, k_Y)$ problem.	53
Figure 5.18	Pareto-sets for Zone3 scenario in $F(k_X, k_Y)$ problem	54
Figure 5.19	Pareto-front for Zone2 scenario in $F(k_X, k_Y)$ problem.	54
Figure 5.20	Pareto-sets for Zone2 scenario in $F(k_X, k_Y)$ problem	55
Figure 5.21	Pareto-front for Zone1 scenario in $F(k_X, k_Y)$ problem.	55
Figure 5.22	Pareto-sets for Zone1 scenario in $F(k_X, k_Y)$ problem.	56
Figure 5.23	Pareto-front for Straight Track scenario in $F(k_X, k_Y)$ problem.....	56
Figure 5.24	Pareto-sets for Straight Track scenario in $F(k_X, k_Y)$ problem	57
Figure 5.25	Track shift force values in $F(k_X, k_Y)$	57
Figure 5.26	Derailment coefficient values in $F(k_X, k_Y)$	58
Figure 5.27	Pareto-front for Zone4 scenario in $F(c^P_X, c^P_Y, c^P_Z)$ problem.	59
Figure 5.28	Pareto-sets for Zone4 scenario in $F(c^P_X, c^P_Y, c^P_Z)$ problem.	60
Figure 5.29	Pareto-front for Zone3 scenario in $F(c^P_X, c^P_Y, c^P_Z)$ problem.	60
Figure 5.30	Pareto-sets for Zone3 scenario in $F(c^P_X, c^P_Y, c^P_Z)$ problem.	61
Figure 5.31	Pareto- front for Zone2 scenario in $F(c^P_X, c^P_Y, c^P_Z)$ problem.	61
Figure 5.32	Pareto-sets for Zone2 scenario in $F(c^P_X, c^P_Y, c^P_Z)$ problem.	62

Figure 5.33	Pareto-front for Zone1 scenario in $F(c^P_X, c^P_Y, c^P_Z)$ problem.	62
Figure 5.34	Pareto-sets for Zone1 scenario in $F(c^P_X, c^P_Y, c^P_Z)$ problem.	63
Figure 5.35	Pareto-front for Straight Track scenario in $F(c^P_X, c^P_Y, c^P_Z)$ problem..	63
Figure 5.36	Pareto-sets for Straight Track scenario in $F(c^P_X, c^P_Y, c^P_Z)$ problem. ..	64
Figure 5.37	Track shift force values in $F(c^P_X, c^P_Y, c^P_Z)$	64
Figure 5.38	Derailment coefficient values in $F(c^P_X, c^P_Y, c^P_Z)$	65
Figure 5.39	Initial and final value of wear objective function.....	66
Figure 5.40	Initial and final value of comfort objective function.....	66

List of Tables

Table 2.1	Wz Ride Comfort classification [Sperling (1941)] [Sperling and Betzhold (1956)].	7
Table 2.2	Ride Comfort classification [CEN (1999)].	9
Table 2.3	Categories for the Wear number.	11
Table 3.1	Railway model body composition.	20
Table 3.2	Wheel properties.	21
Table 3.3	Rail properties.	21
Table 3.4	Material properties.	21
Table 4.1	Curve track classification according to Banverket BVF 586.41.	29
Table 4.2	Curve track scenarios	30
Table 4.3	Scenarios for reference assessment.	32
Table 5.1	Optimization algorithm settings.	39
Table 5.2	Design parameters boundaries and initial value in $\Gamma_{WEAR}(k_X, k_Y)$ optimization.	40
Table 5.3	Wear optimized values for each operational scenario in $\Gamma_{WEAR}(k_X, k_Y)$.	41
Table 5.4	Optimized longitudinal stiffness for each operational scenario in $\Gamma_{WEAR}(k_X, k_Y)$.	42
Table 5.5	Optimized lateral stiffness for each operational scenario in $\Gamma_{WEAR}(k_X, k_Y)$.	43
Table 5.6	Comfort values in $\Gamma_{WEAR}(k_X, k_Y)$.	44
Table 5.7	Design parameters boundaries and initial values in $\Gamma_{WEAR}(c^P_X, c^P_Y, c^P_Z)$ optimization.	45
Table 5.8	Wear optimized values for each operational scenario in $\Gamma_{WEAR}(c^P_X, c^P_Y, c^P_Z)$.	46
Table 5.9	Optimized longitudinal damping coefficient for each operational scenario in $\Gamma_{WEAR}(c^P_X, c^P_Y, c^P_Z)$.	47
Table 5.10	Optimized lateral damping coefficient for each operational scenario in $\Gamma_{WEAR}(c^P_X, c^P_Y, c^P_Z)$.	48
Table 5.11	Optimized lateral damping coefficient for each operational scenario in $\Gamma_{WEAR}(c^P_X, c^P_Y, c^P_Z)$.	49
Table 5.12	Comfort values in $\Gamma_{WEAR}(c^P_X, c^P_Y, c^P_Z)$.	50
Table 5.13	Computation time for each optimization.	65

Notations

Roman upper case letters

$B(f)$	Frequency weighting function.
C_x^p	Primary longitudinal damping (Ns/m).
C_y^p	Primary lateral damping (Ns/m).
C_z^p	Primary vertical damping (Ns/m).
C_x^s	Secondary longitudinal damping (Ns/m).
C_y^s	Secondary lateral damping (Ns/m).
C_z^s	Secondary vertical damping (Ns/m).
\bar{E}	Energy dissipation (Nm/m).
F_ξ	Longitudinal creep force (N).
F_η	Lateral creep force (N).
F	Force (N).
J_x^{bf}	Bogie frame longitudinal moment of inertia (kgm^2).
J_z^{bf}	Bogie frame vertical moment of inertia (kgm^2).
J_z^w	Wheelset vertical moment of inertia (kgm^2).
K_x^p	Primary longitudinal stiffness (N/m).
K_y^p	Primary lateral stiffness (N/m).
K_z^p	Primary vertical stiffness (N/m).
K_x^s	Secondary longitudinal stiffness (N/m).
K_y^s	Secondary lateral stiffness (N/m).
K_z^s	Secondary vertical stiffness (N/m).
$L_{l,m}$	Transition curve length (m).
M_ζ	Spin moment (Nm).
N_{MV}	Comfort index according to UNE-ENV 12299.
$2Q_0$	Mean axle load (kN).
Q	Vertical wheel force (kN).
R	Radius of curvature (m).
$V_{MAX,ADM}$	Maximum admissible vehicle speed (m/s).
$V_{ADM,SERV}$	Maximum admissible service vehicle speed (m/s).
WZ	Wertungszahl, comfort index
ΣY	Track Shift forces (kN).
$\Sigma Y_{max,lim}$	Permissible Track Shift forces (kN).
(Y/Q)	Derailment coefficient.

Roman lower case letters

a_0	Acceleration amplitude measured at floor level (m/s^2).
a^{wrms}	Root-mean-square value of frequency-weighted acceleration (m/s^2).
$a_{iP95}^{W_{aj}}$	95% of the root-mean-square value of the frequency-weighted acceleration (m/s^2).
a_y	Track plane acceleration (m/s^2).
b_0	Half distance for definition of track cant (m)
d	Linear damping coefficient (Ns/m).
g	Acceleration of gravity (m/s^2).
h_d	Cant deficiency in circular curve (m)
h_t	Cant elevation (m)
k	Linear stiffness (N/m).
k_1	Constant in Track Shift forces equation.
l_0	Initial spring length (m).
l_F	Final spring length (m).
$m^{\text{axle box}}$	Axle box mass (kg).
m^{cb}	Car body mass (kg).
m^w	Mass of the wheelset (kg).
m_{veh}	Vehicle mass (kg).
n	Number of axles of the vehicle.
v_ξ	Longitudinal sliding velocity (m/s).
$v_{lim,km/h}$	Permissible speed (km/h).
v	Vehicle velocity (m/s).
v_η	Lateral sliding velocity (m/s).
v_{ij}	Damper velocity along the line of action (m/s).

Greek letters

Δh_t	Difference in cant elevation (m).
Δh_d	Difference in cant deficiency in circular curve (m).
v_η	Lateral creep in contact plane wheel-rail.
v_ξ	Longitudinal creep in contact plane wheel-rail.
Γ	Objective function.
Φ	Spin.

Abbreviations

GA	Genetic Algorithm
MBS	Multi body Simulation.
RMS	Root mean square

1 Introduction

1.1 Research background and aims

Along the historical development of railways as a mean of transportation, the year 1903 must be pointed out as one of its milestones with respect to achieved velocity. In that year the top speed of 210km/h has been achieved during a test run in Berlin [López, A. (2004)]. After eighty years, in 1983 the first European high-speed railway passenger line connected Paris and Lyon. It is clear that the operating speed has been one of the most prominent aspects that attracted more attention from researchers. Running the vehicle on higher speeds has several advantages. For instance, it gives the possibility to reduce the track access charges and as a result operating costs. It also helps to transport the passengers faster and make the railway vehicles competitive with other types of transportation like aeroplane or passenger cars. Therefore, increasing the operating speed has been a priority with the aim to maintain the railway as one of the most widely used means of transportation.

Nevertheless, once dealing with higher values of velocity, important factors like ride comfort and/or safety are forced to suffer from relevant degradation which in critical cases can lead to undesired situations such as a derailment. As a consequence, it is extremely important for the railway companies to consider the ride comfort and safety issues during the operation. In this regard, several standards have been developed during the past few decades in different countries to guarantee the ride comfort and safety of the railway operation. Nowadays, some of the trains are provided with special mechanisms that allow reaching speeds up to 380km/h without risking the lives of the passengers.

One of the most important elements that can affect the behaviour of a railway vehicle at high speeds (especially on curved tracks) is the suspension system and its corresponding components. In this way, along the past two centuries many researchers have designed several suspension systems and control strategies in order to improve the vehicle performance. From the very first version of bogie in H-shaped frame to the recent bogie frame models equipped with the ultimate semi-active and active suspension technology, passing through the development of the passive suspension approach which led to a simple but reliable suspension chosen by most of the railway manufacturers for their vehicles.

Moreover, in the course of the railway vehicles' suspension system development, singular mechanisms have been designed with the purpose of improving the tactics used by a rail vehicle while approaching a curve. For example, the tilting technology [Goodall, R. (1999)] has added to the classic primary and secondary suspension configuration a significant help to increase the ride comfort and safety on curves.

As aforementioned, active suspension systems can improve the vehicle performance (especially ride comfort). However such systems need more advanced components like sensors, actuators and additional power supplies which increase the design, operation and maintenance costs. Passive systems on the other hand, can significantly affect in a positive manner the ride comfort, safety and wear in railway operations. But the problem with such strategy is that the suspension coefficients remain unchanged during the operation and thus it is vital to choose suitable values to have the optimized performance.

Consequently, it is really important to formulate and solve several optimization problems for a given railway vehicle to detect the optimized values of design parameters (primary and secondary spring and dampers in the case of suspension system) to achieve the optimized performance of the vehicle. This could be done by the optimization routines through the computer simulations. It should be noted that the vehicle performance in railway industry can be defined in many different ways and there are several factors and parameters that can affect the vehicle performance. Vehicle speed, ride comfort, safety, wear, track access charges, fatigue, maintenance cost are some of these parameters. Based on each combination of those parameters one can propose a new definition for the vehicle performance. In the present study, speed, ride comfort, safety and wear are the most important parameters that determine the vehicle performance. It is usually desirable to run the vehicle as fast as possible to reduce the track access charges while having low wear and a satisfactory level of ride comfort and safety in the system.

Having in mind all these, the importance of the activities carried out by the railway engineers is clear. Nonetheless, the railway as a mean of transportation has nowadays aspects in which the improvement is a must in order to remain as a respectable adversary against airplane and automobile.

1.2 Literature review

During the last decades the rail vehicle industry has undergone a great development in terms of security, reliability and quality. Due to this progress the high speed rail vehicle is nowadays considered as a competent and cost-effective source of transport in comparison with the car and air transport. Unfortunately, as the speed of travel increases the oscillatory movements of the vehicle become higher and that could negatively affect the three parameters under study in this project, *i.e.* safety, ride comfort and wheel-rail wear [Wang, Liao (2003)]. Therefore, it is absolutely necessary to have this in mind during the design stage of new vehicles in order to have an optimum level of those functions during the operation.

As a starting point to understand the behaviour of a rail vehicle and the corresponding effects on the ride comfort, safety and wear it is necessary to investigate different linear and nonlinear system dynamic responses. The critical hunting speed as the origin of the instabilities of a rail vehicle as well as the effects of the wheel conicity, the wheel-rail contact and the track imperfections have been studied thoroughly in [Fan and Wu (2006)]. To overcome the negative effects of such parameters on the above mentioned objectives functions, several suspension systems and control strategies have been proposed.

Traditionally, the suspension strategy used in railway vehicles was based on the employment of spring and oil dampers. This type of passive approach is characterized by a high level of simplicity, low-price and the absence of external power supply. Through the careful selection of the suspension design parameters, engineers tried to obtain a compromise between the performances of the vehicle in both straight and curved tracks. Moreover, the critical hunting speed and instability problem with respect to the maximum admissible speed of the vehicle is presented [Dukkipati and Guntur (1984)].

With the development of the control technology is demonstrated that this trade-off between vehicle's performance in straight and curved track can be solved by the implementation of active actuators [Mei and Goodall (2000)]. If the passive strategy is not able to deal with the high frequency disturbances from the track irregularities, the active one compensates such limitations with the use of active devices governed by algorithms that determine the best properties for each operational scenario [Jalili (2001)].

By the use of special dampers based on controllable fluids (Magneto-Rheological dampers), several semi-active suspension approaches are characterized by a low level of energy requirement as well as low cost [Goodall, Mei et al (2003)]. This technology can be considered as the next step after the passive one since when constant electrical current circulates, the Magneto-Rheological (MR) damper behaves like the passive case.

The suspension strategy that takes the advantage of the fully active technology provides the optimal damping response in each time step. The drawbacks of this configuration are the high level of complexity concerning the control method and the high level of energy requirements [Orvnäs (2011)]. Because of this, such technology has been applied mainly in the secondary suspension with the aim of improving the ride comfort.

The last type of the new suspension strategies applied on railway vehicles is the so called tilting technology. It is focused on the reduction of the lateral acceleration excess when negotiating a curve [Anderson, Berg and Stichel (2007)]. This technology can be based on passive and active actuators and has led to a substantial increase of the velocity on curves. Examples of this technology are the TALGO train (Spain) in the passive case and the ETR-450 “Pendolino” (Italy) or the X2000 (Sweden) in the active one.

As aforementioned, most of the semi-active and active suspension systems are more complicated than the corresponding passive techniques and of course need medium to high design and maintenance costs. Passive systems on the other hand can significantly improve the performance and are still a point of interest. However, it is extremely important to formulate and solve several optimization problems to be able to get the best performance out of such systems. In [Johnsson, Berbyuk, Enelund, (2012)] a multiobjective optimization with respect to comfort and safety is performed on passive damping elements of both primary and secondary suspension of a railway vehicle obtaining suspension parameters that improve the default performances. And in [Mousavi, Berbyuk (2013)] a multiobjective optimization problem is contemplated and solved with respect to ride comfort, safety and wear having as design parameters the primary and secondary passive dampers obtaining optimized solutions for different tangent and curved track scenarios at maximum admissible speed.

1.3 Purpose of the project

This project is focused on the dynamics and primary suspension optimization of a high – speed rail vehicle bogie with the aim of improving the following objective functions: safety, ride comfort and rail – wheel wear, while running the vehicle at the maximum admissible speed on different operational scenarios.

For this purpose, a simple but reliable railway model is created in the multi-body simulation (MBS) software SIMPACK as well as five different operational scenarios from very small radius curve to the tangent track and with measured data for the track irregularities. The modelling results from each operational scenario are verified against the limit values available in several railway standards.

Based on the previous study [Suarez B., Mera J.M., Martinez M.L. and Chover J.A. (2012)], an optimization of the longitudinal and lateral stiffness of the passive primary suspension has been carried out with the intention of minimizing the rail – wheel wear objective function, while ride comfort and safety levels are taken into account as thresholds. In order to perform the optimizations, genetic algorithm (GA) based routines in MATLAB are chosen and Simat module in SIMPACK is used to connect the MATLAB Simulink and SIMPACK environments. This procedure will be fully discussed later on.

The optimized values of the primary springs obtained in the previous part are used in the second problem to optimize the primary dampers in the longitudinal, lateral and vertical directions with respect to wear on the same operational scenarios.

For the next step a bi-objective optimization problem to reduce wear and increase the ride comfort level is formulated and the primary springs and dampers are optimized with respect to the new conditions in a similar manner described earlier.

The results of the optimized passive primary suspension, can significantly improve the vehicle performance. Furthermore, the primary passive damper case can give some hints when designing the semi-active suspension strategies using on/off switching, skyhook or other techniques which can even provide better performances.

2 Objective Functions

As described earlier the fundamental aim of this project is to optimize the primary suspension system components in order to improve the railway performance. Therefore, it is necessary to present the mathematical formulation of the objective functions to be used in the optimization routines.

An improvement in railway performance achieved during the optimization in this project is quantified in better values of wheel-rail wear, ride comfort and ride safety objective functions. This chapter explains how these three quality indexes are accurately evaluated.

2.1 Ride comfort

One of the most important aspects that any type of transportation must ensure is an acceptable level of comfort perceived by the passengers. However, it is a complicated parameter to be measure since it is not defined only by means of physically quantifiable quantities but also by subjective perceptions of each passenger.

Among all the possible measureable features that define the ride comfort level in railways, the most widely used in the normative is the value of accelerations inside the car [Anderson, Berg and Stichel (2007)].

2.1.1 Wertungszahl (Wz)

This comfort index was defined by the German researchers Sperling and Betzhold and it is based on the measurement of the accelerations on the floor of the car body [Sperling (1941)] [Sperling and Betzhold (1956)]. This index is determined by the equation (2.1):

$$Wz = [100 \cdot B(f) \cdot a_0]^{0.3} \quad (2.1)$$

Where, a_0 is the acceleration amplitude (m/s^2) at floor level in the lateral or vertical direction and $B(f)$ is the frequency weighting function.

The frequency weighting functions used in this index are defined so that the passenger is considered to be more affected by frequencies in the range 3 to 7 Hertz. In this way, the next figure shows the frequency weighting functions in vertical and lateral directions used in Wz ride index, see Figure 2.1.

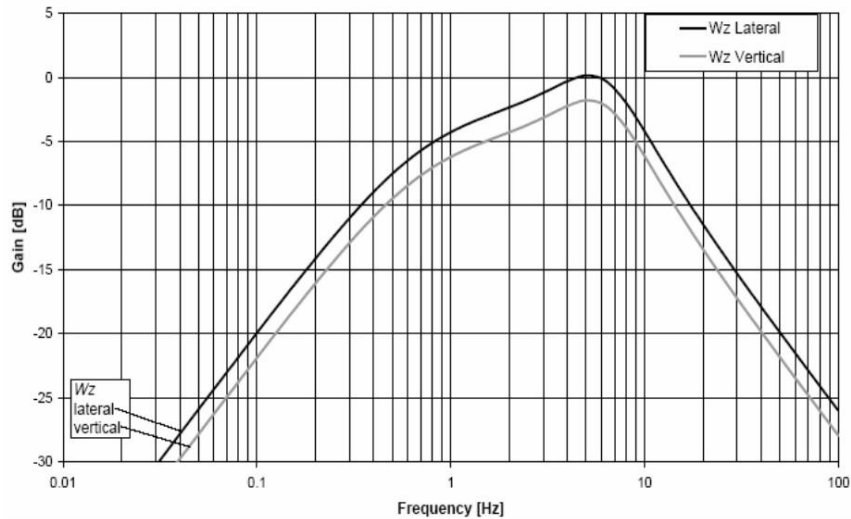


Figure 2.1 Frequency weighting functions for Wz [Sperling and Betzhold (1956)].

Nonetheless, the Wz index can be also computed according to equation (2.2) [Sperling (1941)] [Sperling and Betzhold (1956)]:

$$Wz = 4.42 \cdot (a^{wrms})^{0.3} \quad (2.2)$$

Where, a^{wrms} makes reference to the root-mean-square value of the frequency-filtered accelerations.

Finally, the level of comfort when using the Wz approach is defined in Table 2.1.

Table 2.1 Wz Ride Comfort classification [Sperling (1941)] [Sperling and Betzhold (1956)].

Ride Index Wz	Comfort level
1	Just noticeable
2	Clearly noticeable
2.5	More pronounced but not unpleasant
3	Strong, irregular, but still tolerable
3.25	Very irregular
3.5	Extreme irregular, unpleasant
4	Extremely unpleasant. Harmful

2.1.2 UNE – ENV 12299

Another approach to determine the comfort level in railways is described by The European Committee of Normalization in the document EN-12299. Taking into account the standards UIC-513 and ISO-2631, two hierarchical approaches are defined [CEN (1999)].

The first one, characterized by not being compulsory, regards the accelerations inside the vehicle measured not only at the vehicle's floor but also at the passenger's seat in the three directions. Moreover, it takes into consideration the effects of the curve transitions and discrete events.

The second one is declared as mandatory in the standard and defined as a simplified method based on measurements of acceleration on the floor of Mean Comfort. It is calculated using the equation (2.3)

$$N_{MV} = 6 \cdot \sqrt{(a_{XP95}^{W_{ad}})^2 + (a_{YP95}^{W_{ad}})^2 + (a_{ZP95}^{W_{ab}})^2} \quad (2.3)$$

Where $a_{iP95}^{W_{aj}}$ stands for the 95% of the root-mean-square (rms) value of the frequency weighted accelerations (m/s^2) measured at floor level in the three directions. The rms value must be computed over periods of five seconds in order to take into account the lowest frequencies.

The weighting functions recognize the vibrations at frequencies in the range from 0.5 to 80 Hz as the main interval affecting the passengers. Figure 2.2 and Figure 2.3, show the weighting functions used for each direction.

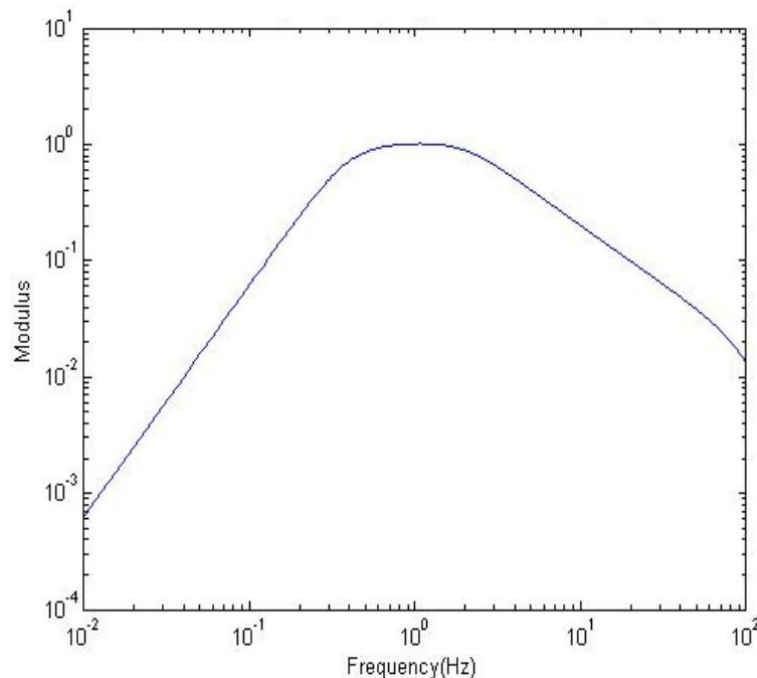


Figure 2.2 Frequency weighting functions for Wad [CEN (1999)].

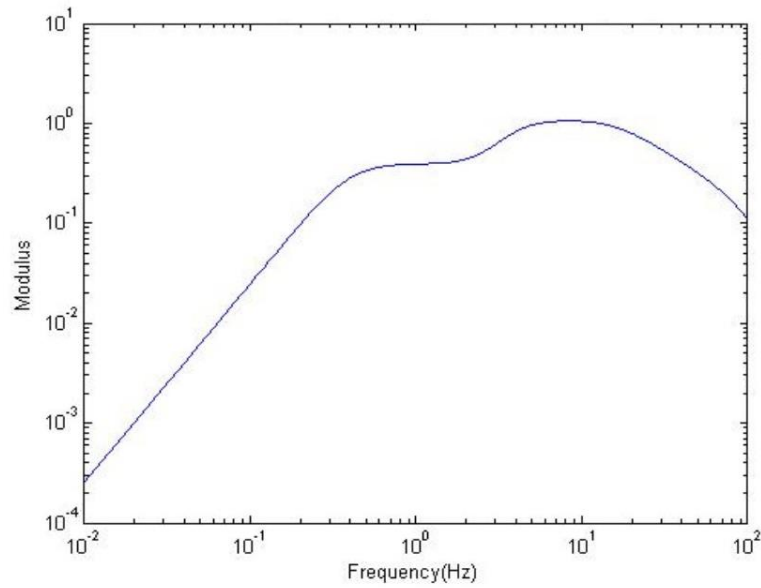


Figure 2.3 Frequency weighting functions for Wab [CEN (1999)].

The scale to estimate the ride comfort level is shown in Table 2.2.

Table 2.2 Ride Comfort classification [CEN (1999)].

$N_{MV} < 1$	Very comfortable
$1 \leq N_{MV} < 2$	Comfortable
$2 \leq N_{MV} < 4$	Medium
$4 \leq N_{MV} < 5$	Uncomfortable
$N_{MV} \geq 5$	Very uncomfortable

According to the standard, to properly determine the ride comfort index in a railway vehicle, the value of the mean comfort must be calculated in three points along the railway vehicle, particularly above each bogie and at the centre of the vehicle.

This second approach is the one selected to compute ride comfort objective function in this project.

2.2 Safety

Apart from the ride comfort index, another aspect that compromises the passenger's integrity is the level of the railway vehicle safety. Without any kind of hesitation, this parameter has to be scrupulously studied until acceptable levels are achieved.

In this way and following the EN-14363 standard [CEN (2005)], the safety of a rail vehicle is assessed by means of two quantities: the track shift forces and derailment coefficient.

2.2.1 Track shift forces

The first parameter that quantifies safety deals with the lateral forces created due to the wheel-rail contact as the vehicle runs over the track. This is particularly important because a high value of track shift forces leads to track irregularities (which increases the maintenance costs) and in the latest case to a derailment.

Equation (2.4) defines how to calculate this value for the leading wheelset [CEN (2005)]:

$$\sum Y_{20\text{Hz},2\text{m},\text{mean},99.85\%} \leq k_1 \left(10 + 2Q_0/3 \right) \text{ (kN)} \quad (2.4)$$

Where k_1 is a constant factor and $2Q_0$ is the mean axle load of the vehicle defined by equation (2.5):

$$2Q_0 = \frac{m_{veh}g}{n} \quad (2.5)$$

Where m_{veh} is the mass of the vehicle, g the gravitational force and n is the number of axles of the vehicle.

The final value of the track shift forces is equal to the 99.85% of the value obtained from filtering the forces with a sliding mean over 2m in 0.5m increments and a 20 Hz low-pass filter.

2.2.2 Derailment coefficient

Another factor that must be taken into account while analysing the railway safety is the parameter that quantifies the risk of derailment. It is called derailment coefficient and is defined with equation (2.6) [CEN (2005)]:

$$\left(Y/Q \right)_{20\text{Hz},2\text{m},\text{mean},99.85\%} \quad (2.6)$$

Where Y and Q represent the lateral and vertical forces for the wheel-rail contact under study, respectively. As can be seen the final value is equal to the 99.85% of the value obtained from filtering the quotient with a sliding mean over 2m in 0.5m increments and a 20 Hz low-pass filter.

To obtain a representative value, this parameter must be computed with respect to the leading outer wheel according to the standard.

2.3 Rail–wheel wear

The last design parameter used to characterize the economic aspects of a railway vehicle considered in this work is the so called rail–wheel wear and is related to the change of geometry of both wheel and rail profiles due to the contact forces and corresponding wear present in the contact patch between both elements.

The contact formulation used here is governed by non-linear equations and the theory behind the contact forces, the corresponding creepages in the contact patch and the wear produced is rather complicated and out of the focus in this project. In this way, several approaches are present in the literature explaining with more or less accuracy the loss of material present in the above mentioned contact.

For the purpose of this project, a simple but widely accepted approach of the wear computation has been adopted [Orvnäs (2011)] [Johnsson, A., Berbyuk, V., Enelund, M. (2012)] [Mousavi, M., Berbyuk, V.(2013)]. It is based on the assumption that the wear present in the rail-wheel contact is linearly related to the energy dissipated in the process.

The energy dissipated is defined by equation (2.7):

$$\bar{E} = F_{\xi} \cdot v_{\xi} + F_{\eta} \cdot v_{\eta} + M_{\zeta} \cdot \Phi \quad (2.7)$$

Where F_{ξ}, F_{η} are the creep forces in the longitudinal and lateral directions and M_{ζ} is the spin moment. Moreover, v_{ξ}, v_{η} and Φ are the corresponding creepages. The longitudinal and lateral creepages are defined by equations (2.8) and (2.9):

$$v_{\xi} = \frac{v_{\xi}}{v} \quad (2.8)$$

$$v_{\eta} = \frac{v_{\eta}}{v} \quad (2.9)$$

Where v_{ξ} and v_{η} are the sliding velocities in the longitudinal and lateral directions, respectively and v is the vehicle speed.

Once in equation (2.9), the spin creepage contribution is dismissed, the result is called the *wear number*.

The rms value of the wear number in the leading outer wheel is the parameter used to quantify the wear objective function in this project and is given by equation (2.10):

$$\Gamma_W = \sqrt{\frac{1}{t_f - t_0} \int_{t_0}^{t_f} (F_{\xi} \cdot v_{\xi} + F_{\eta} \cdot v_{\eta})^2 dt} \quad (2.10)$$

According to [Pearce and Sherratt (1991)] this objective function is classified as Table 2.3 illustrates:

Table 2.3 Categories for the Wear number.

$Wear\ Number < 100$	Low
$100 \leq Wear\ Number < 200$	Medium
$Wear\ Number \geq 200$	High

3 SIMPACK modelling

In order to perform the computer simulations, a suitable model have to be created first. This could be done using different Multi Body Simulation software. In this project, one of the most well-known software accepted by industrial and academic communities called Multi Body Simulation (MBS) software SIMPACK rail module is used. It should be noted that SIMPACK 9.4 version is used for both modules, Pre and Post-Processor.

Along the next sections a detailed explanation of how to create a railway model in SIMPACK is given as well as a detailed explanation of the railway model used in this project.

3.1 Modelling in SIMPACK v9.4 rail module

The MBS software SIMPACK v9.4 allows the user to create a railway model with different levels of complexities including large number of degrees-of-freedom, different types of suspension elements, several contact models, wheel and rail profiles, and so on. SIMPACK rail module is known as one of the best computer simulation environments which together with the possibility of importing measurement data provides a relatively cheap and reliable package for design and verification of new or modifying the existing rail models by the industry.

3.1.1 “Rail - Wheel Pair” panel

The first step to create a SIMPACK rail model is the specification of the number of wheelsets composing the railway model. By doing this, the user is asked to fulfil the panel “Rail-Wheel Pair” in which the contact between rail and wheel is defined for each wheelset.

As can be seen in Figure 3.1, this panel is divided into five tabs by which properties such as rail and wheel profile, material parameters or friction coefficient have to be defined.

In the “Wheel” tab, the main aspects asked by the software are the wheel profile (S1002 used in this project) as well as the nominal wheel radius and lateral distance between wheels.

Concerning the “Rail” tab, the type of rail profile (UIC 60 for this project) and the rail cant (inward inclination of the rail with respect to the vertical plane) are asked.

In “Contact, Normal Force” tab, the user is asked to define the theory used to calculate the normal contact forces. For this project the contact type “Hertzian” is selected as recommended by SIMPACK.

Finally in “Tangential Forces” tab, the type of theory by which the tangential contact forces are computed is defined. Even though SIMPACK provides several options, for this project the FASTSIM algorithm has been used for being a simplified version of the nonlinear contact theory. It calculates the contact forces in different directions in a fast and reliable way which is suitable when performing optimization routines.

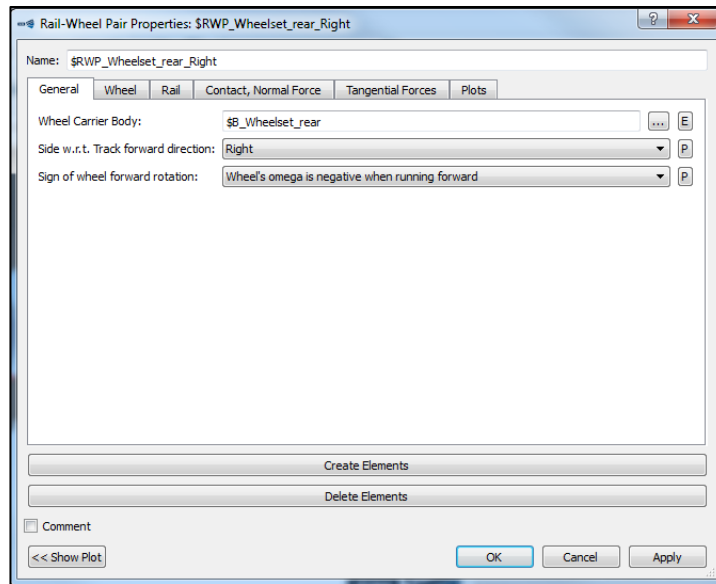


Figure 3.1 “Rail-Wheel Pair” panel

3.1.2 “Track Pair” panel

When each rail–wheel pair is defined, SIMPACK asks to specify the left and right hand contact pairs corresponding to each wheelset. In this way, as can be seen in Figure 3.2, important features as the track gauge and the equivalent conicity are defined. For this project, the value of the equivalent conicity is set to 0.186, being a widely used value in correspondence to the track gauge and type of wheel profile used in this project [Andersson, E., Berg, M., Stichel, S. (2007)].

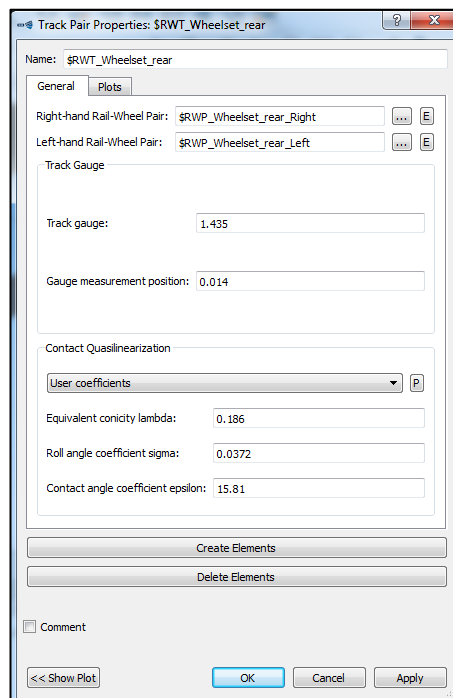


Figure 3.2 “Track Pair” panel.

3.1.3 “Rail – Wheel Contacts” panel

The last step concerning the evaluation of the contact problem is the definition of the method to calculate the tangential contact forces and spin contact torque. In SIMPACK library [SIMPACK (2013)] are seven different approaches available and as described earlier the most common rail-wheel contact algorithm in SIMPACK called “FASTSIM” is chosen here.

3.1.4 Bodies

In order to build up the model, it is necessary to introduce the different geometries that compose the model apart from the wheelsets. This is done with the help of the “Body Properties” panel as can be seen in Figure 3.3:

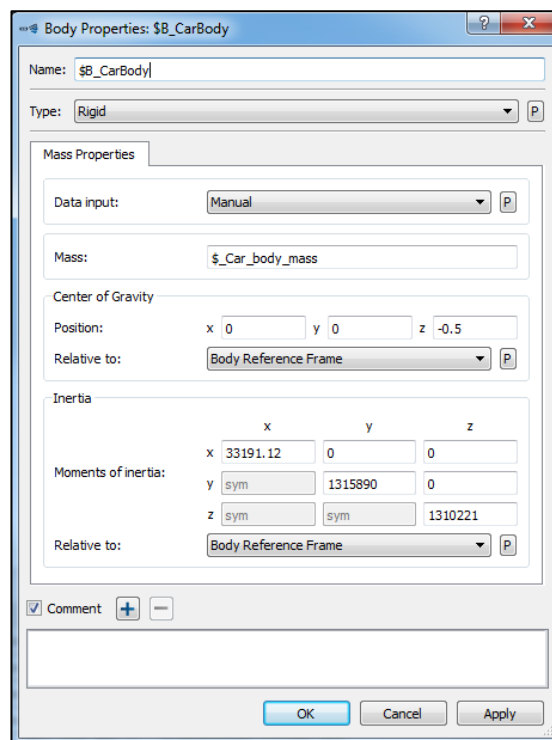


Figure 3.3 “Body properties” panel.

By fulfilling the body properties panel (manually or from a specified file) mass, moment of inertia and other properties corresponding to each body of the model are defined.

It should be noted that SIMPACK gives the possibility of building a model from multiple sub-models, also called *Substructures*. In this way, one can create the bogies in a separate SIMPACK file, for example and import the bogies in the main model as substructures to simplify the modelling process.

3.1.5 Track definition

Once the rail-wheel contact has been totally defined as well as each body composing the model, the next step is the definition of the scenario in which the model will be positioned. In order to do this, a new track has to be created.

As can be seen in Figure 3.4 a “Rail” track is defined by two tabs.

In the first one the user is asked to specify the length and curvature of different sections composing the track in the horizontal plane, as well as the superelevation and the differences in the vertical direction.

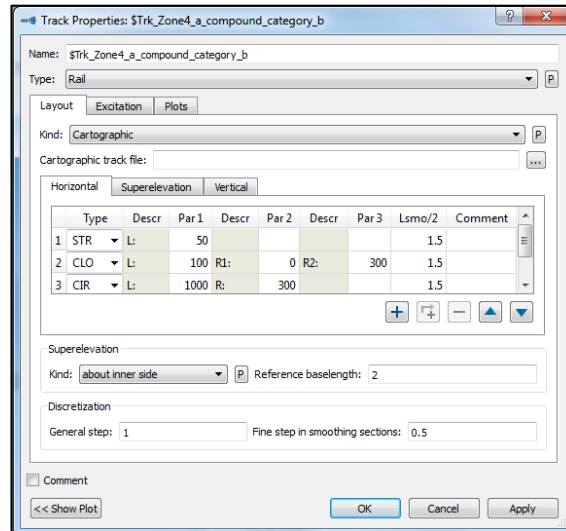


Figure 3.4 “Track Properties - Layout” panel

The second tab is dedicated to the introduction of the track irregularities, see Figure 3.5. It should be noted that in this work measured track data in lateral, vertical, roll and gauge directions is used as track irregularities in different operational scenarios

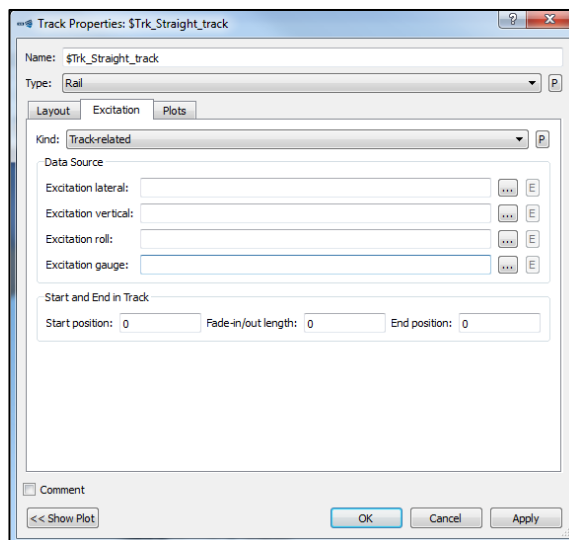


Figure 3.5 “Track Properties - Excitation” panel

3.1.6 Static equilibrium and preload calculation

Once the railway model is completely defined along with the scenario, it is time to prepare it for the simulations.

With this aim a static initial position must be determined. In such situation, all the derivatives of the state equations (velocities and accelerations) defining the mechanical system are zero. Moreover, special attention must be paid to the elastic force elements present in the model.

With the help of the “Preload Calculation” menu, SIMPACK calculates the value of the preload of every suspension element taking charge of the effect of the gravity on different masses.

In Figure 3.6, the preloads values for each force element can be seen. Moreover, the “Maximum residual acceleration” of the model is also specified in this menu, and of course the corresponding number at the equilibrium position must be equal to zero or very small. For the illustrated case, this value is smaller than 0.012 rad/s^2 , so can be said that the effect of the gravity is absorbed by the force elements.

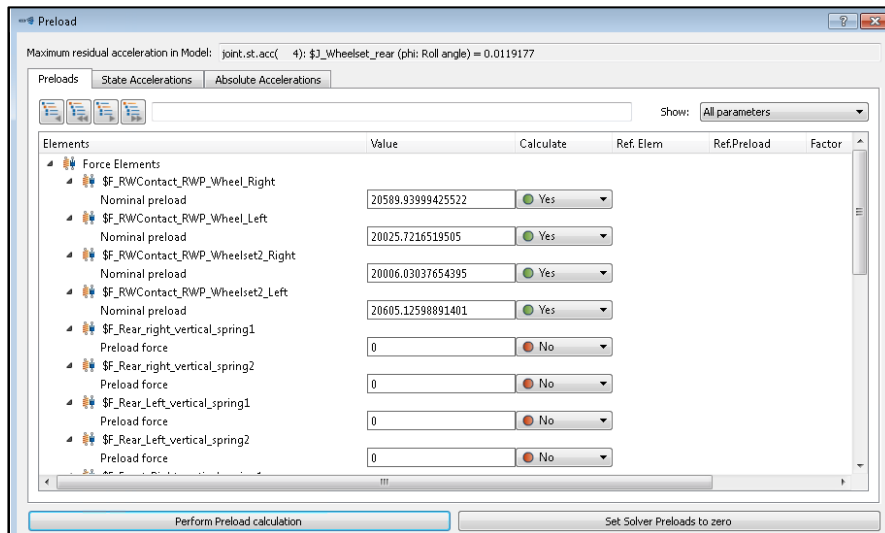


Figure 3.6 Preload calculation menu.

Once the force elements are in equilibrium, it is time to determine the equilibrium position of the full model in the three directions. To do so, SIMPACK provides the tool “Static Equilibrium” which calculates the static position of each body and gives the “Maximum force residuum” in that position. This value, as in the previous case for the “Preload calculation”, must be equal to zero or very small.

In Figure 3.7 the “Static equilibrium” panel for the model under analysis is shown.

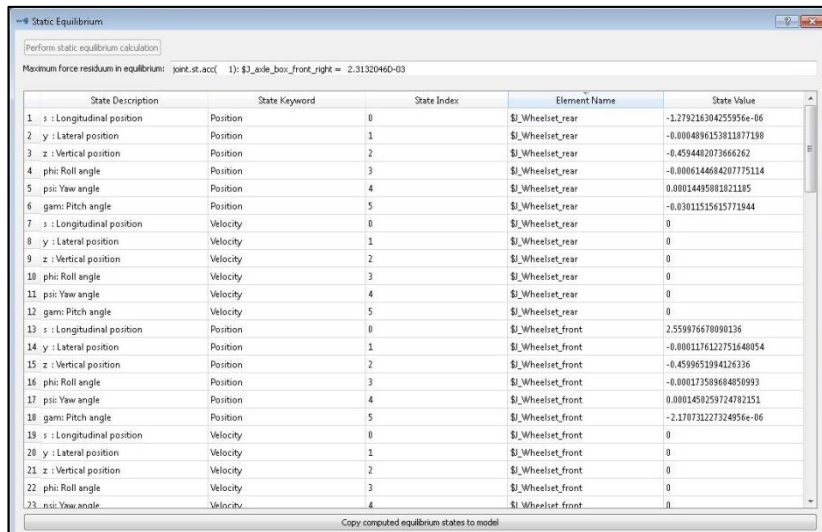


Figure 3.7 Static equilibrium menu.

Finally, once SIMPACK finds a suitable equilibrium position, the model is ready to be used in the simulations.

3.1.7 “Solver Settings” panel: time integration off-line and on-line

The final step in the creation of a SIMPACK model is the introduction of the characteristics that define the selected solver. All the options are gathered in the “Solver Settings” panel.

The “Solver Settings” board is divided into fourteen tabs which provide several solver possibilities as can be seen in Figure 3.8.

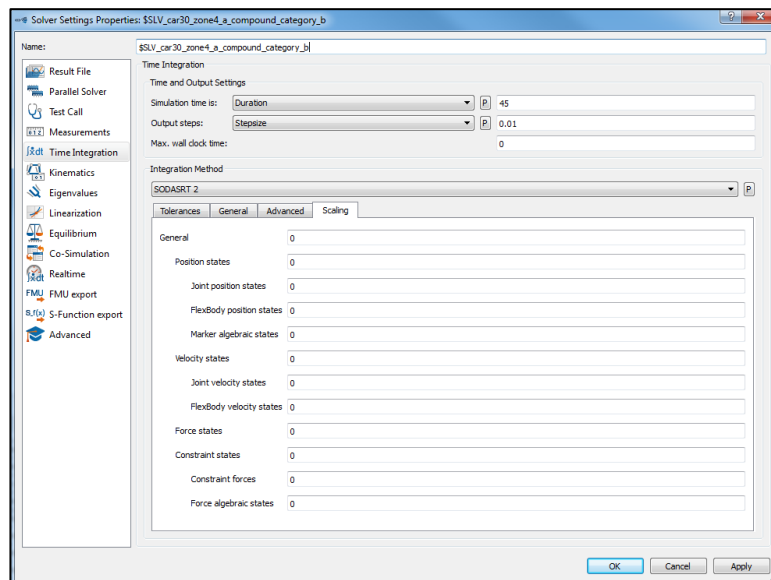


Figure 3.8 “Solver Settings” panel.

In this way, important aspects as the result file name, simulation time and the integration method and its tolerances are introduced here in this panel. It is also possible to apply the desired measurement settings in this module. Since, all the objective functions defined in previous chapter are a function of carbody accelerations, contact forces and in general the dynamics response of the system, it is really necessary to activate the corresponding measurement options in this panel to be able to use them later on in the objective function evaluation and optimization.

There are two sets of simulations available in SIMPACK called on-line and off-line. If the user has intention to examine that the model behaves properly in the scenario selected, the button “Time Integration - On-line” can be clicked. In this way, the dynamic behaviour of the model can be seen in SIMPACK pre-processor environment. The off-line time integration option on the other hand can perform the simulations and the necessary measurements at the same time and is used in the optimization routines implemented in this work.

For more information concerning MBS software SIMPACK v9.4 see SIMPACK documentation.

3.2 Railway vehicle model created for the simulations

In order to study the dynamics and optimization of the suspension system of a railway vehicle, a one-car model is created for this project using SIMPACK v9.4.

Since the optimization problem is a time consuming process, the approach followed is to create and use a simple but reliable model. Of course there are several possibilities for the suspension system configuration and one can use different combinations of passive springs and dampers as the primary and secondary system. Here, a suspension system configuration based on the one available in [Cheng, Lee, Chen (2009)] is selected and thus created in SIMPACK.

Figures 3.9 and 3.10 show the front and top views of one bogie and the corresponding primary and secondary suspension system set up used in the model. From these figures, it is clear that there are parallel spring-dampers in the longitudinal, lateral and vertical directions working as the primary and secondary suspension system for this model.

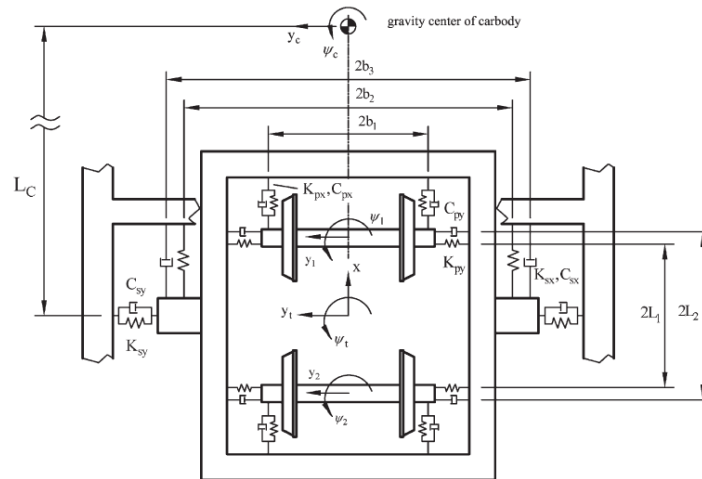


Figure 3.9 Top view of reference railway model [Cheng, Lee, Chen (2009)].

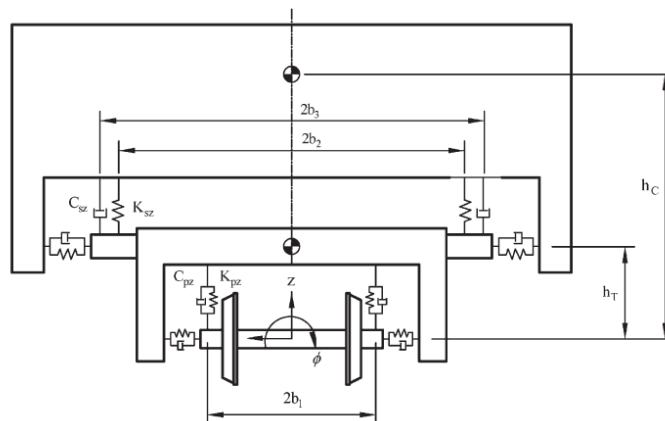


Figure 3.10 Front view of reference railway model [Cheng, Lee, Chen (2009)].

Moreover the model created for the simulations is composed by the following bodies, see Table 3.1. It should be noted that all bodies are considered to be rigid bodies.

Table 3.1 Railway model body composition.

Body Name	Quantity	Total degree-of-freedom
Car body frame	1	6
Bogie frame	2	12
Wheelset	4	24
Axle box	8	8

It is clear that, all the bodies have the full degrees of freedom (6 DOF in space), except for the axle box which has only one, being this the rotation with respect to the lateral axis. Therefore and as it can be computed, the model used during the simulation has 50 DOF.

The next figures, see Figures 3.11, 3.12 and 3.13, show how the model created looks like.

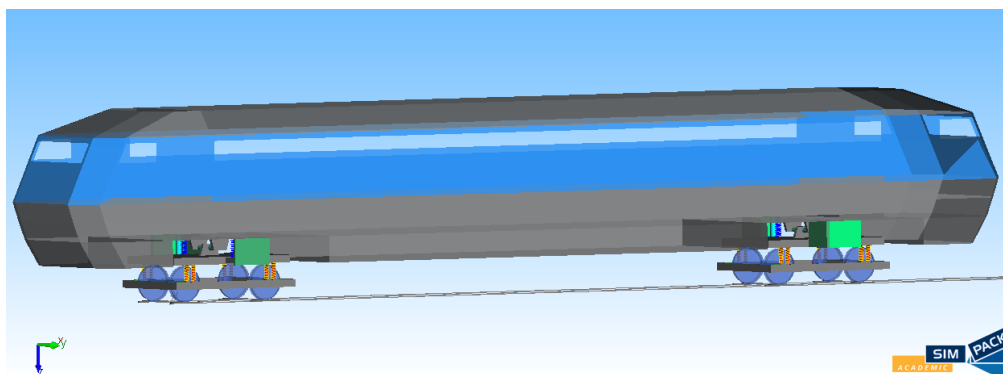


Figure 3.11 Railway model used during the simulations.

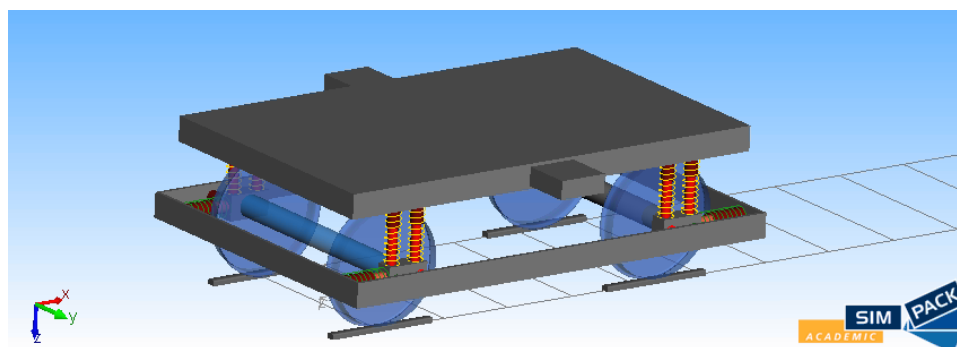


Figure 3.12 Bogie frame connected to wheelsets by the primary suspension.

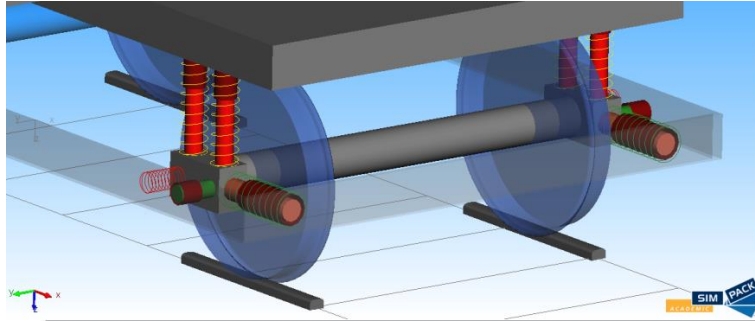


Figure 3.13 Detail of the primary suspension.

3.2.1 “Rail – Wheel pair” panel–Railway vehicle model

As mentioned before in Section 3.1.1, the “Rail-Wheel pair” panel is dedicated to define the characteristics of the rail-wheel contact. In the case of the railway model created, those features are resumed in Tables 3.2, 3.3 and 3.4:

Table 3.2 Wheel properties.

Profile	S1002
Nominal radius	0.46m

Table 3.3 Rail properties.

Profile	UIC60
Rail cant	1:40

Table 3.4 Material properties.

Young modulus (GPa)	210
Poisson number	0.25
Kinematic coefficient of friction	0.45

Every other aspect considered in this panel was defined as in the configuration recommended by SIMPACK.

3.2.2 “Track Pair” panel–Railway vehicle model

For the case of the railway model the track-pair properties are defined as follow:

- Track gauge: 1.435m.

3.2.3 “Rail – Wheel contacts” panel–Railway vehicle model

As described earlier, the algorithm used in the railway model to calculate the tangential forces and the tangential torque is called “FASTSIM” (A Fast Algorithm for the Simplified Non-Linear Theory of Contact). It is based on the method of Kalker and assumes that the contact patch is elliptical and divided into elements. Thus, calculates the contact forces stresses by a simplified numerical integration.

This algorithm has been selected because is well-accepted in vehicle dynamics calculations and more importantly provides fast and reliable results. Note that the spin contact torque is not calculated for the wear analysis.

3.2.4 Track definition–Railway vehicle model

In this section only the track irregularities used during the simulations are explained. The different scenarios in which the simulations take place are explained afterwards in Chapter 4.

The track irregularities employed in the simulations come from real data measured in the high-speed train track that joins the Swedish cities of Göteborg and Stockholm.

The track irregularities data is divided into four excitations: lateral, vertical, roll and gauge. Figures 3.14, 3.15, 3.16 and 3.17 represent the track irregularities in the four directions for the first 100 metres.

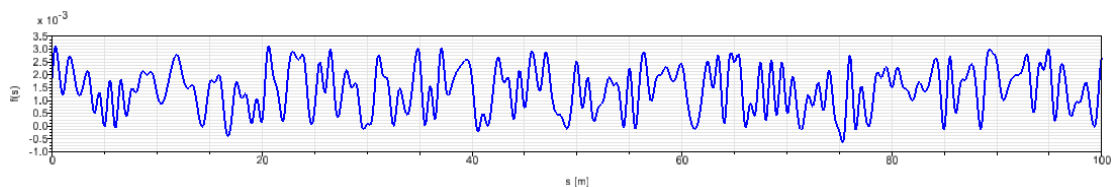


Figure 3.14 Track irregularities in lateral direction.

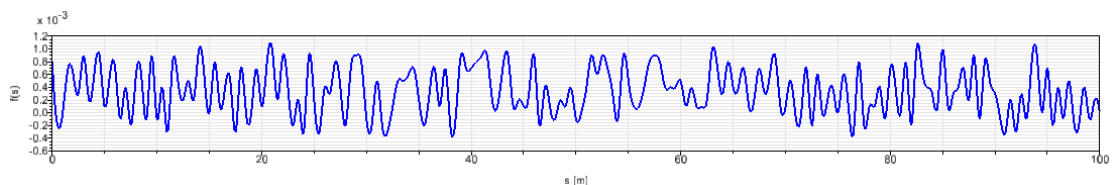


Figure 3.15 Track irregularities in vertical direction.

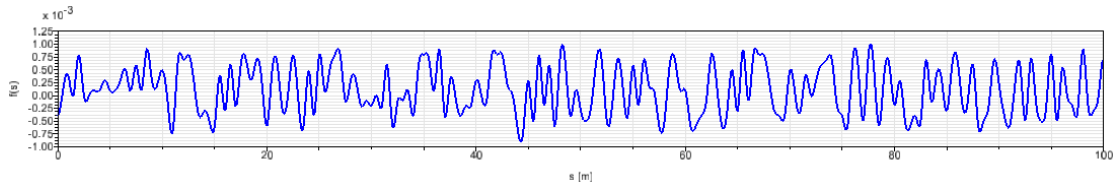


Figure 3.16 Track irregularities in gauge direction.

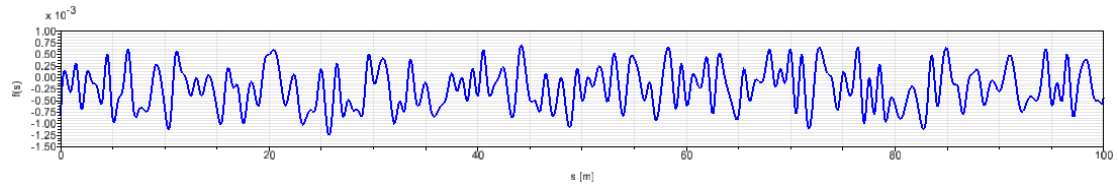


Figure 3.17 Track irregularities in roll direction.

3.2.5 “Solver Settings” panel – Railway vehicle model

Taking into account that the “Solver Settings” panel includes specific aspects for each scenario, in this section only the common features to every scenario are defined.

- Time Settings.
 - Step size: 0.01s.
 - Integration method: SODASRT 2 (recommended by SIMPACK)
 - General absolute tolerances: $1 \cdot 10^{-5}$.
 - General relative tolerances: $1 \cdot 10^{-10}$.

3.2.6 Railway vehicle model description–Engineering model

The values that define the mechanical properties of each body composing the railway vehicle model in this project are close to the ones utilized in a high speed railway vehicle.

3.2.7 Railway vehicle model suspension strategy: primary and secondary suspension

The suspension configuration used in the model of this project is divided into two different levels: primary and secondary suspension.

The primary suspension works as the connection between the wheelsets (axle box) and the bogie frames. In this manner, the vibrations and forces coming from the wheel–rail contact are absorbed by elastic couplings and energy dissipater elements on the three directions. In the same way, the secondary suspension connects the bogie frames with the car body frame.

For the case of the railway model under study, both the primary and secondary suspensions are composed by linear parallel springs and dampers oriented on the longitudinal, lateral and vertical directions as can be seen in Figures 3.18 and 3.19.

Must be noted that even though in reality most of the railway vehicles use a rigid bar as the longitudinal element of the primary suspension, in this project springs and dampers are used in order to vary their properties in a simpler way.

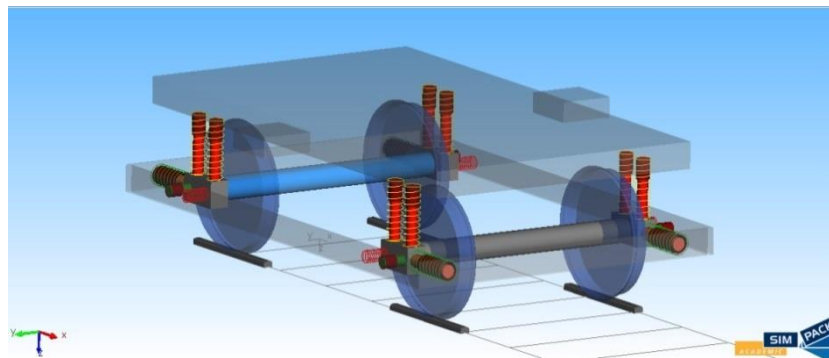


Figure 3.18 Primary suspension.

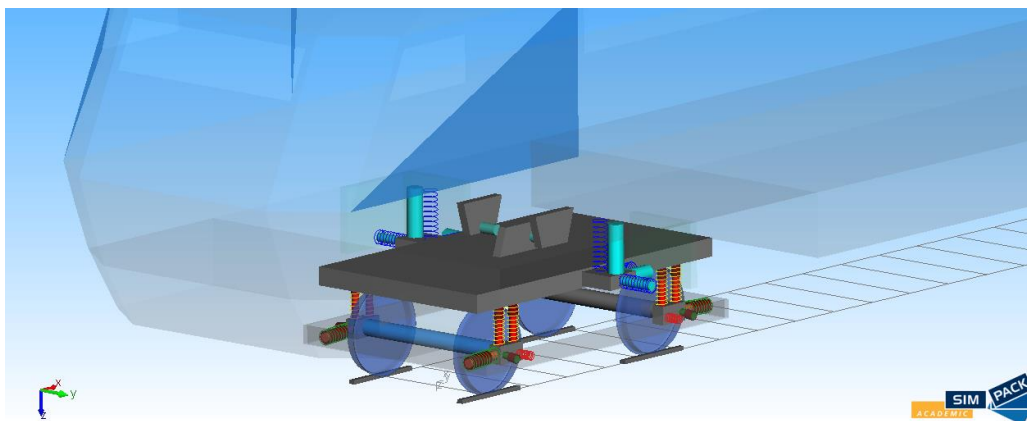


Figure 3.19 Secondary suspension.

With the aim of having the simplest but still reliable suspension strategy, the spring elements are modelled in SIMPACK with the force element “Type 1 – Spring PtP (Point - to - Point)”. This type of force element is the simplest available in SIMPACK library and it is characterized by creating a force law along the line of action between the two points to be connected. The force law for these massless springs is defined according to equation (3.1):

$$F = k * (l_F - l_0) \quad (3.1)$$

Where, F stands for the force applied [N], k is the linear stiffness of the spring [N/m] and l_F and l_0 are the final and initial spring length [m] respectively.

This type of force element does not take into account the effects of the moment created by a lateral offset between the points to connect and the force law is not referred to a specific direction but just to the line of action.

With respect to the type of damper used in this model, the force element “Type 2 – Damper PtP” has been chosen. It corresponds to the simplest energy dissipater element available in SIMPACK. Thus, it creates a force law between the points to connect according to equation (3.2):

$$F = d * v_{ij} \quad (3.2)$$

Where F is making reference to the damping force [N], d stands for the linear damping coefficient [Ns/m] and v_{ij} stands for the damper relative velocity along the line of action [m/s].

Finally this type of force element is considered massless and it does not take into account lateral moments produced by lateral offset between the points to connect.

Additionally to the abovementioned elements, the suspension strategy used in this model is completely defined by the introduction of a pair of bumpstops located in both front and rear bogies with the aim of reducing the lateral displacement of the car frame with respect to each bogie, see Figure 3.20.

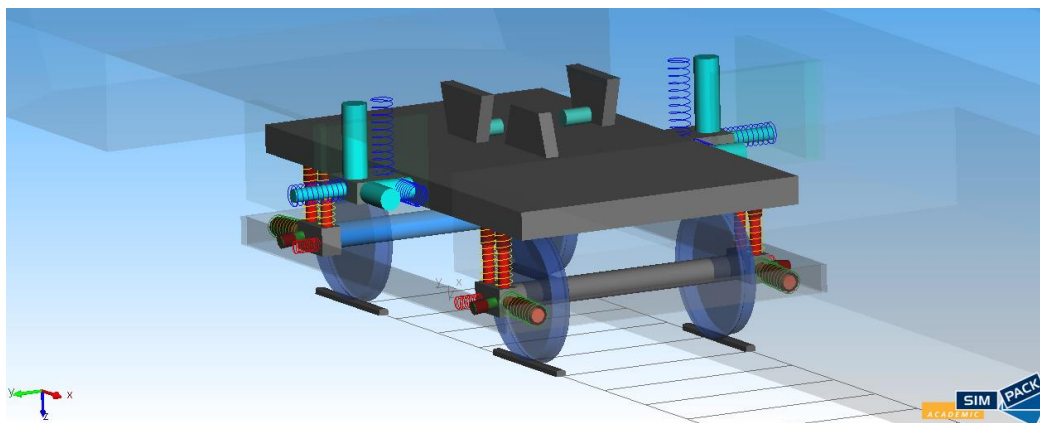


Figure 3.20 Bumpstop force element located between rear bogie and car frame.

These two bumpstops are equal and modelled by the force element “Type 5 - Spring-Damper Parallel Cmp”. The nonlinear force law that governs these elements can be seen in Figure 3.21:

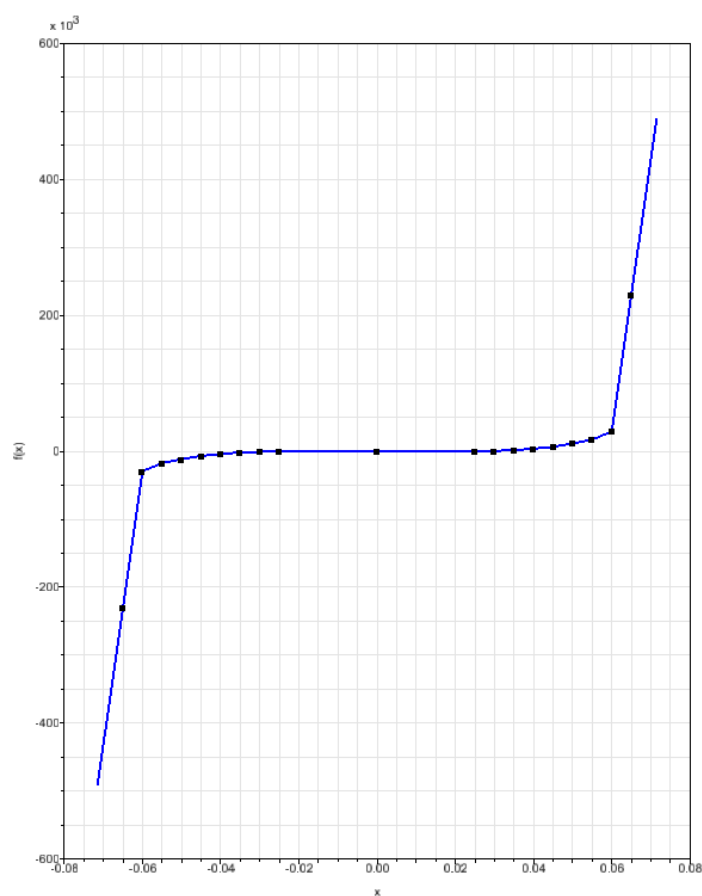


Figure 3.21 Bumpstop function [x axis (m), y axis (N)].

As can be seen in the previous picture, the function that defines the bumpstop is very non-linear and characterized by a strong intensification as the displacement grows.

Finally the values of the linear stiffness and damping coefficients that define the suspension system of the railway vehicle model under study in this project are chosen to be similar to the values use in a high speed railway vehicle.

4 Reference model assessment and verification

With the aim of having a reference model to compare with the results obtained from the optimization of primary passive components, this chapter is dedicated to the evaluation of the dynamics response and objective functions of the railway vehicle model created using the initial guess of the passive suspension values.

4.1 Operational scenarios for the reference assessment

The first step in the creation of a reference model is the description of the operational scenarios. For this aim to be achieved, the following points explain the properties and specifications of different operational scenarios.

4.1.1 Straight track scenario

As can be seen in Figure 4.1 the straight track scenario is characterized by a 1000 meters long track and the vehicle speed is set to be 275km/h. This last value comes from the standard EN-14636 in which it is defined that the speed in straight track for the safety assessment must be equal to the maximum admissible speed of the vehicle.

Since the maximum service speed of the vehicle is equal to 250km/h, the maximum admissible speed is defined according to equation (4.1):

$$V_{MAX,ADM} = V_{ADM,SERV} * 1.1 = 275km/h \quad (4.1)$$

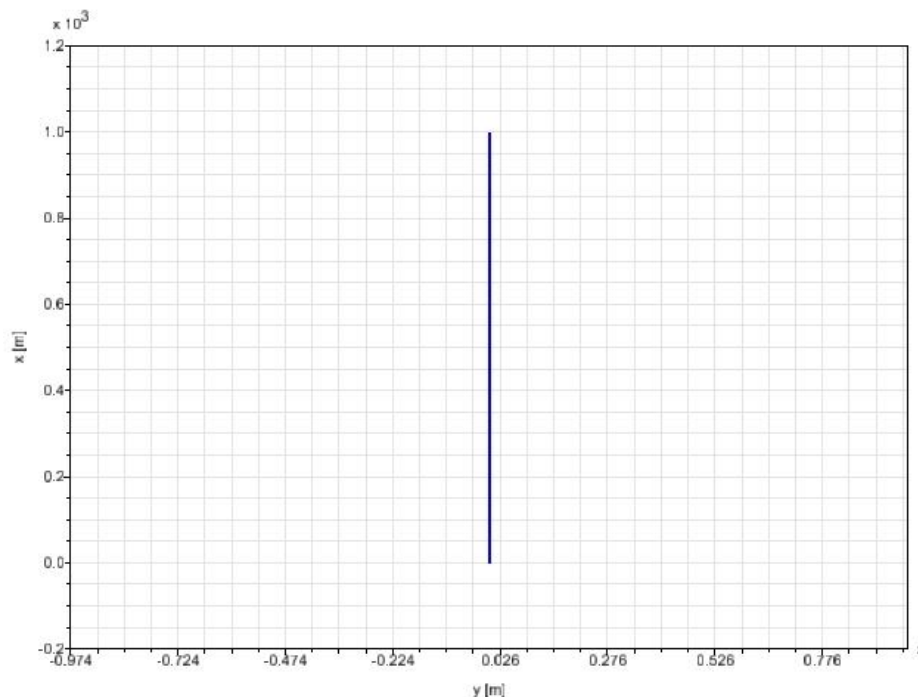


Figure 4.1 Straight track layout representation.

4.1.2 Curved track scenario

The parameters needed to define a curved track are the following: radius of curvature, length, cant elevation and track plane acceleration.

As Figure 4.2 shows, this last factor is defined as the value of the centrifugal acceleration in the horizontal plane created by both rails suffered by the train when negotiating a curve.

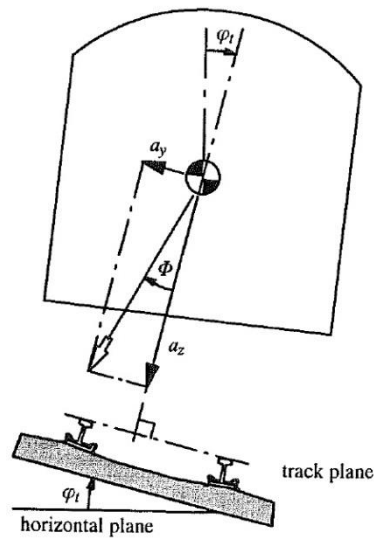


Figure 4.2 Track plane acceleration [Anderson, Berg and Stichel (2007)].

The next equation resumes the mathematical representation of the track plane acceleration, see equation (4.2):

$$a_y = \frac{v^2}{R} - g \cdot \frac{h_t}{2b_o} \quad (4.2)$$

Where v is the vehicle speed, R is the radius of curvature, g is the gravitational force, and h_t and $2b_o$ are the values that define the superelevation and length in the horizontal plane between both rails, respectively. More in detail, these last two parameters are represented in Figure 4.3.

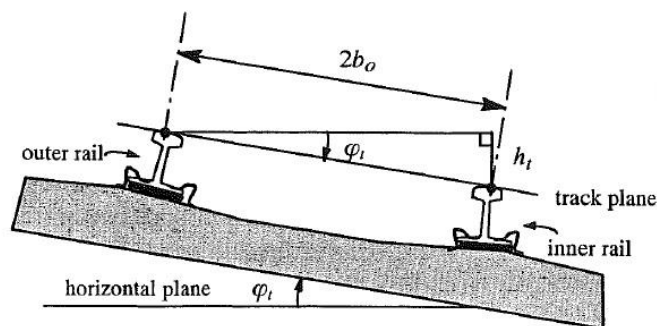


Figure 4.3 Track characteristics [Anderson, Berg and Stichel (2007)].

The track plan acceleration is defined in detail because this parameter is used for the classification of curved track scenarios in the standards.

According to the Swedish Rail Administration standard [Banverket (1996)], the curved track scenarios are categorized in three levels differentiated with respect to the track plane acceleration as can be seen in Table 4.1 [Anderson, Berg and Stichel (2007)]:

Table 4.1 Curve track classification according to Banverket BVF 586.41.

Category	Track plane acceleration ($a_{y,lim}$)	Equivalent cant deficiency ($h_{d,lim}$)
A–Old running gear	0.65m/s^2	0.10m
B–Improved running gear	0.98m/s^2	0.15m
S–SJs tilting trains	1.60m/s^2	0.24m

In this way, every curved scenario prepared for the simulations will be included in category “B–Improved running gear” since the initial passive suspension strategy created in the SIMPACK model is based on the suspension of a vehicle designed for such category. Moreover, in the next sections it will be demonstrated that the model with the initial values of suspension elements satisfies the limits of all the desired objective functions.

To finalize the creation of a curved track, it is necessary to specify the characteristics of the section that connects the initial straight part and the purely curved section. *i.e.* the definition of the transition curve.

This intermediate section is particularly important because it is used to change the rate of cant to the one desired at the corresponding curved track, thus it has an important effect on the ride comfort. According to [Banverket (1996)] for linearly changing value of cant, the following relations are used.

The minimum length of the transition curve is computed by the equation (4.3):

$$\frac{L_{l,m}}{\Delta h_{t,mm}} \geq 0.4 \quad (4.3)$$

Where $L_{l,m}$ is the minimum transition curve length and $\Delta h_{t,mm}$ is the difference of cant at the curved part in millimetres.

The maximum permissible speed at which the railway model can travel along this section is determined as the minimum of the equations (4.4) and (4.5):

$$v_{lim,km/h} \leq \frac{1000 \cdot L_{l,m}}{q_a \cdot \Delta h_{t,mm}} \quad (4.4)$$

$$v_{lim,km/h} \leq \frac{1000 \cdot L_{l,m}}{q_b \cdot \Delta h_{d,mm}} \quad (4.5)$$

Where q_a and q_b are constants and $\Delta h_{d,mm}$ is the cant deficiency. For category “B–Improved running gear” the values of the aforementioned constants are: $q_a = q_b = 5$.

In Table 4.2 the characteristics defining the four curved track scenarios created corresponding to: very small, small, medium and large radius curve are given. Must be noted that the length for every curved track scenario is equal and set to be 1000m.

Table 4.2 Curve track scenarios

Scenario	Radius	Max admissible velocity
Zone 4	300m (Very small radius)	83km/h
Zone 3	600m (Small radius)	117km/h
Zone 2	900m (Medium radius)	144km/h
Zone 1	3200m (Large radius)	240km/h

In the following pictures, see Figures 4.4, 4.5, 4.6 and 4.7, the layouts associated with four curved track scenarios created in this project for the dynamics analysis and optimization are shown.

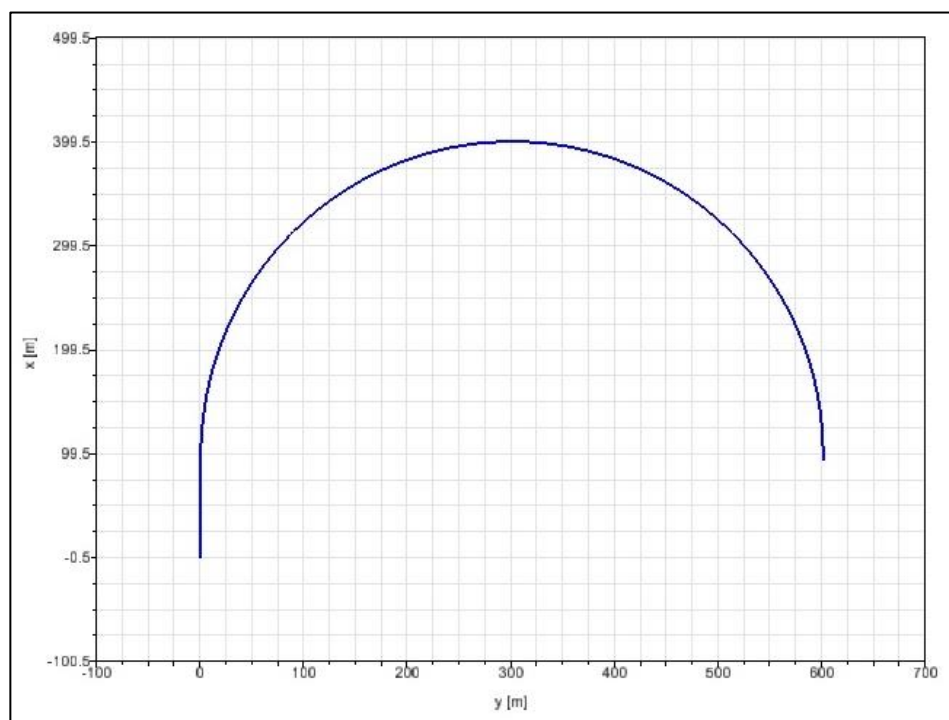


Figure 4.4 Zone 4 curved track layout representation.

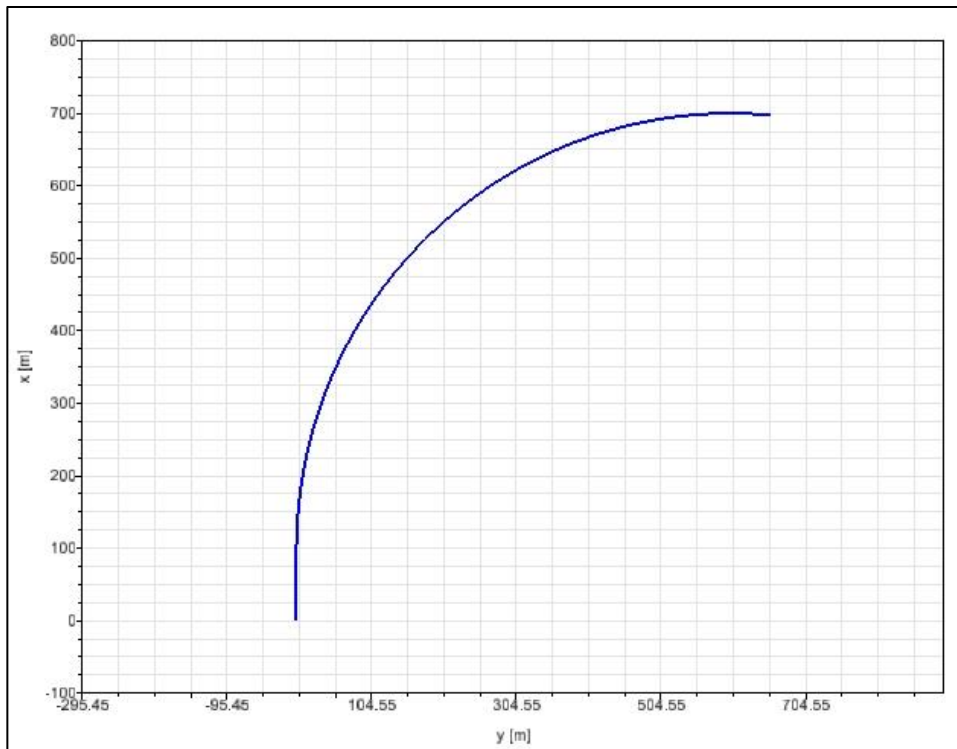


Figure 4.5 Zone 3 curved track layout representation.

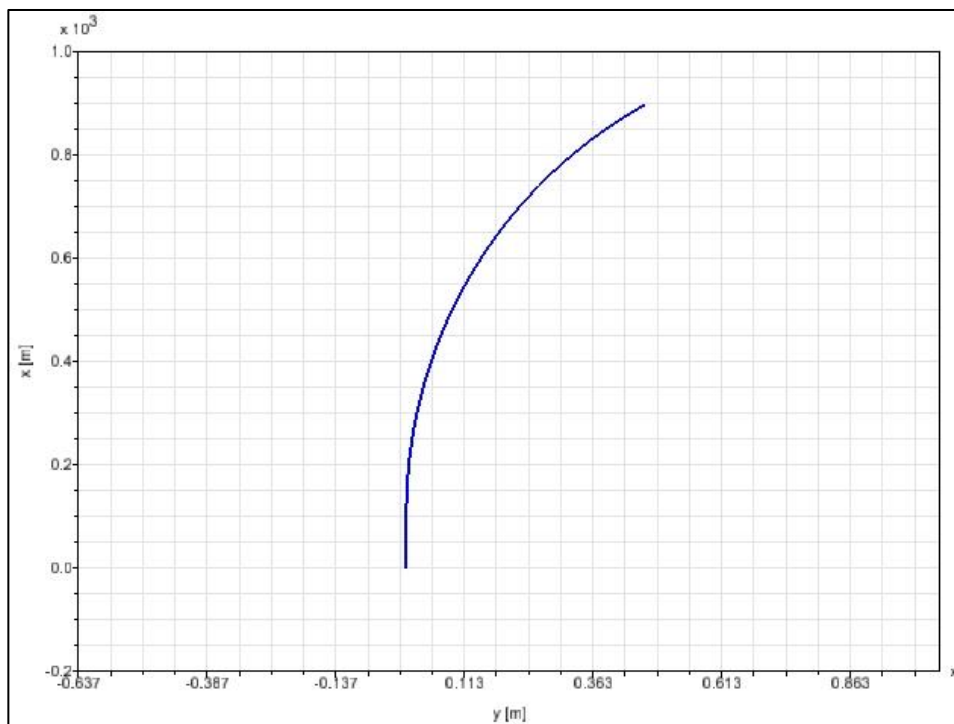


Figure 4.6 Zone 2 curved track layout representation.

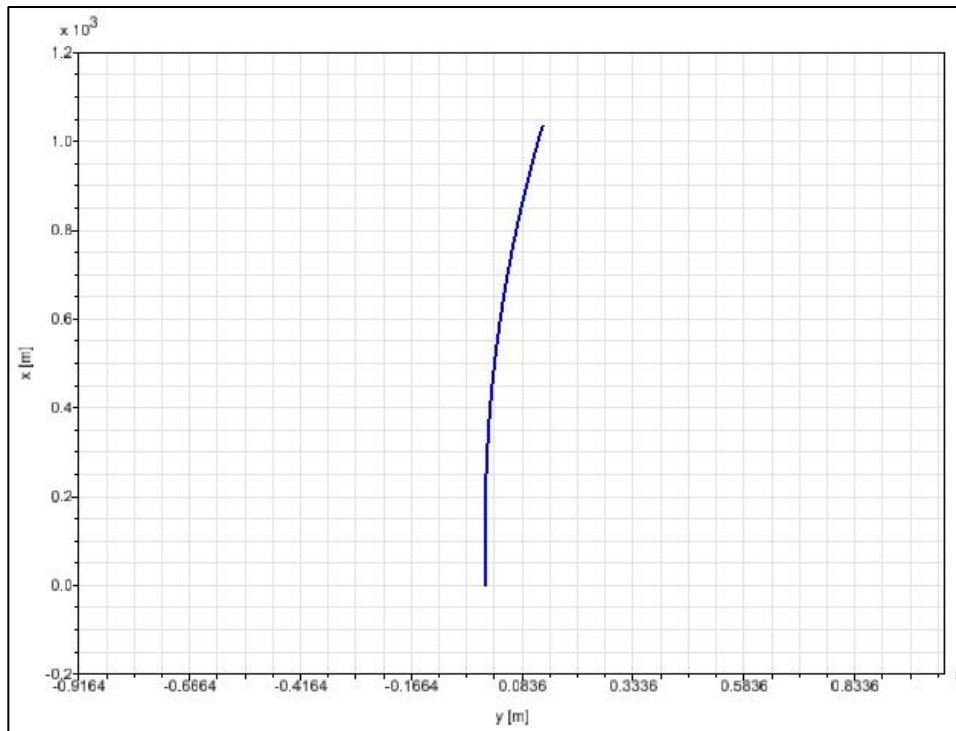


Figure 4.7 Zone 1 curved track layout representation.

4.1.3 Track irregularities

The track irregularities used in each operational scenario are from measured data introduced previously in Chapter 3, in particular Section 3.2.4 and are applied indistinctly in all of the scenarios.

4.1.4 Scenarios for reference assessment – Table resume

Table 4.3 resumes all the scenarios created for the assessment of the reference railway model.

Table 4.3 Scenarios for reference assessment.

Scenario	Radius [m]	Speed [km/h]	Cant [mm]	Track plane acceleration [m/s^2]
Zone 4	300	83	150	0.98
Zone 3	600	117	150	0.98
Zone 2	900	144	150	0.98
Zone 1	3200	240	150	0.98
Straight track	∞	275	-	-

4.2 Reference model assessment-Objective functions evaluation

To finalize Chapter 4, the results in terms of the objective functions obtained during the railway model reference assessment are given and compared with the respective values from standards.

4.2.1 Objective functions limit values

In order to evaluate the results from the reference assessment, it is compulsory to define first of all the limits for each objective function. In this way, the next values illustrate the limits for the three objective functions under study.

- Safety [CEN (2005)]:

- Track shift forces, see equations (2.4) and (2.5).

For the case under study, $2Q_0 = 84.67kN$ and thus, $\Sigma Y_{max,lim} = 38.23kN$ for the leading wheelset.

- Derailment coefficient, see equation (2.6):

- Ride Comfort [CEN (1999)].

The different categories in which the mean value of the ride comfort is divided can be seen in Table 2.2.

- Wear number.

The classification of the wear number values is done according to Table 2.3.

4.2.2 Reference model assessment: Objective functions value

In the following figures, the values obtained during the railway model reference assessment on the five previously mentioned operational scenarios are presented. Note that the horizontal solid line is representing in each case the maximum admissible value or the categories of the objective functions.

- Safety: Track shift forces (Figure 4.8)

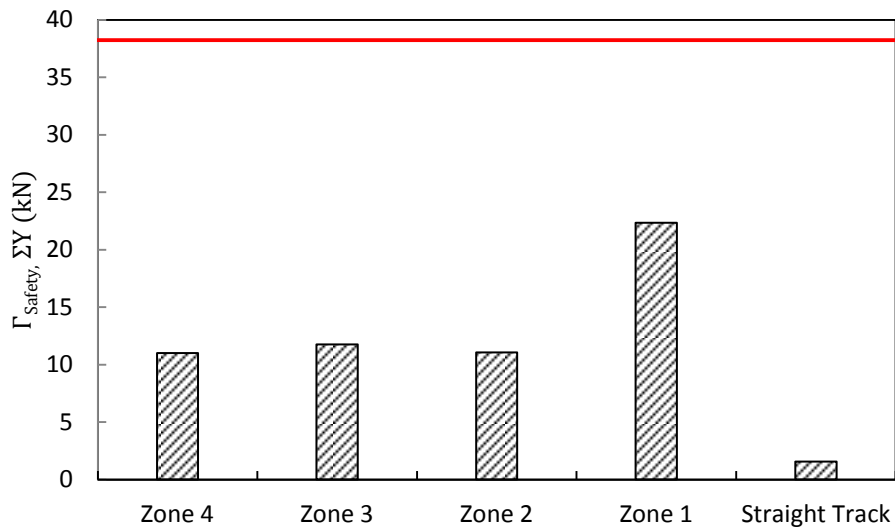


Figure 4.8 Track shift forces for reference assessment.

- Safety: Derailment coefficient (Figure 4.9)

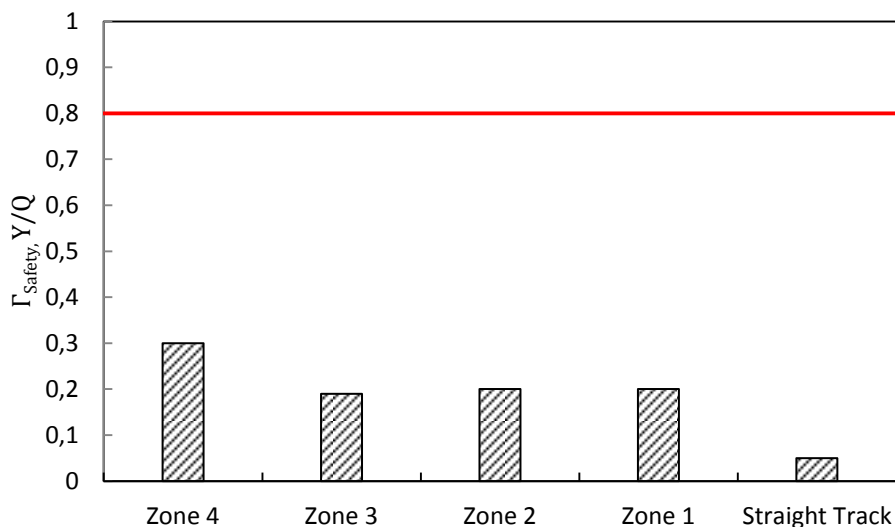


Figure 4.9 Derailment coefficient for reference assessment.

- Ride comfort (Figure 4.10):

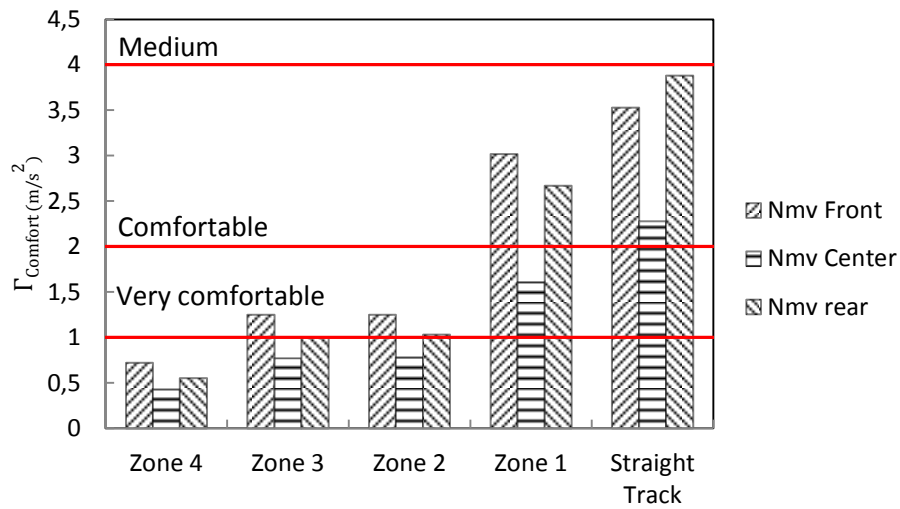


Figure 4.10 Ride comfort for reference assessment.

- Wear number (Figure 4.11):

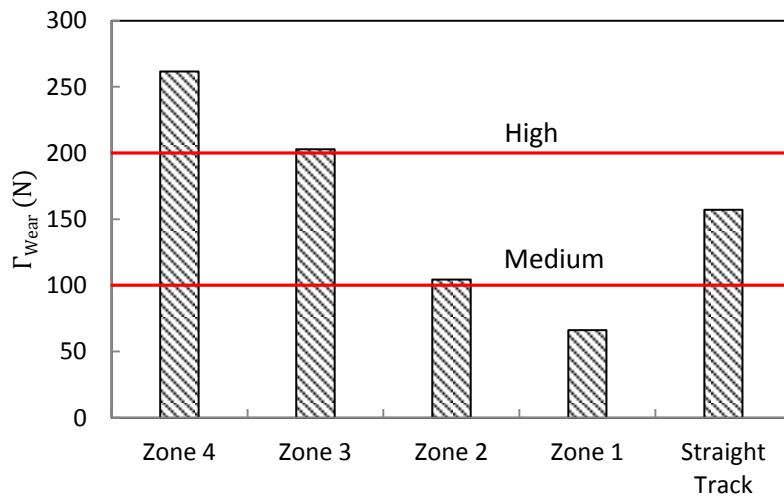


Figure 4.11 Wear number for reference assessment.

As can be seen in the previous tables, all the objective functions are within the admissible ranges (coming from railway standards) for the considered initial guess of the design parameters.

Therefore, the railway model created in SIMPACK introduced in the previous chapters is verified and can be used as a reference model for the optimization of the passive primary suspension system.

5 Optimization, results and discussion

As aforementioned, one of the main aspects that strongly affect the dynamics behaviour of a railway vehicle is the value of those parameters characterizing the suspension system. In this way and especially for the case of passive suspension strategies, the extraction of those parameters leading to the best performance of the railway vehicle model on different operational scenarios is a challenging task that could enhance the comportment of the simplest type of suspension in railways.

To achieve that goal, the optimization routines based on the “Genetic Algorithm” in MATLAB can be employed. However, in order to evaluate the objective functions during the optimization, it is necessary to calculate the dynamics response of the system which has to be done is SIMPACK. Therefore, it is required to connect and run the optimization routine in MATLAB and the SIMPACK model simulations, simultaneously by using Simat block in SIMULINK.

5.1 MATLAB-SIMPACT connection

5.1.1 MATLAB role

The Genetic Algorithm (GA) based optimization routines in MATLAB is known as a powerful optimization tool proposed by many researchers [Baumal, A.E., McPhee, J.J. and Calamai, P.H. (1996)]. As described earlier the optimization routine which includes updating the parameters and evaluating the objective functions should be implemented in MATLAB environment. This procedure is described more in detail in the following.

1. The first task written in the MATLAB code is the introduction and updating the design parameter values. This is done by means of the modification of a sub variable (SubVar) file.

Such files are defined to include different unchanged parameters (for example mass, moment of inertia, stiffness, damping and so on) and can be loaded into a SIMPACK model. Moreover, this type of file has a “.sys” format and can be modified by different types of text editors. Since the optimization routine works in a loop and the value of the design parameters must be updated in each loop, it is necessary to write the corresponding values in a SubVar file to be loadable by SIMPACK in each iteration.

2. When the Subvar file is updated and closed, MATLAB starts a new simulation by calling SIMPACK through the SIMAT block in SIMULINK.

This step constitutes the first part of the MATLAB – SIMPACK connection

3. Once the simulation performed in SIMPACK is finalized and the system dynamics response evaluated, the results are stored in the y-Outputs and send back to MATLAB where by applying different filters and mathematical operations, the value of the objective functions are calculated. Thus, the second part of the MATLAB-SIMPACT connection through SIMULINK is implemented here.

In SIMPACK, a *y-Output* is the mechanism used to export the selected simulation results to the SIMULINK environment.

5.1.2 SIMULINK role

As described earlier, SIMULINK represents the necessary environment to make the MATLAB-SIMPACT connection possible.

SIMULINK is also responsible of launching SIMPACK simulation using the SIMAT block and sending the results of interest obtained from SIMPACK simulations back to MATLAB.

5.1.3 SIMAT Block

The SIMAT block is used as the interface between SIMPACK and SIMULINK as shown in Figure 5.1:

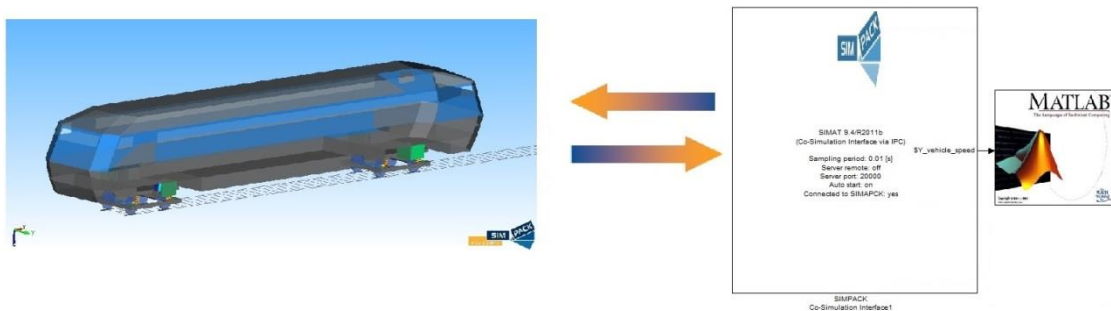


Figure 5.1 SIMULINK – SIMPACK connection by the use of the SIMAT block.

For example, Figure 5.2 shows how a SIMAT block exports the SIMPACK simulations results (creep forces and sliding velocities in this case) to SIMULINK as a part of a wear calculation process. This SIMULINK file could be executed by a MATLAB optimization routine to minimize wear in the system.

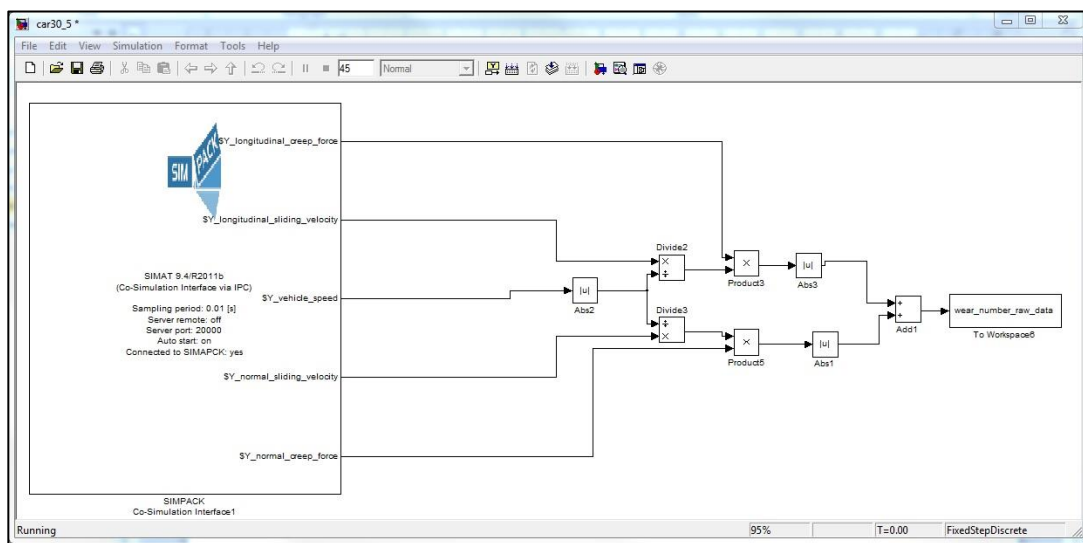


Figure 5.2 SIMAT block in a SIMULINK file.

Once using a SIMAT block, special attention must be paid to the specification of the corresponding SIMPACK model, the simulation time and the tolerances of the solver utilized. All these parameters are defined in the SIMAT block interface as shown in Figure 5.3:

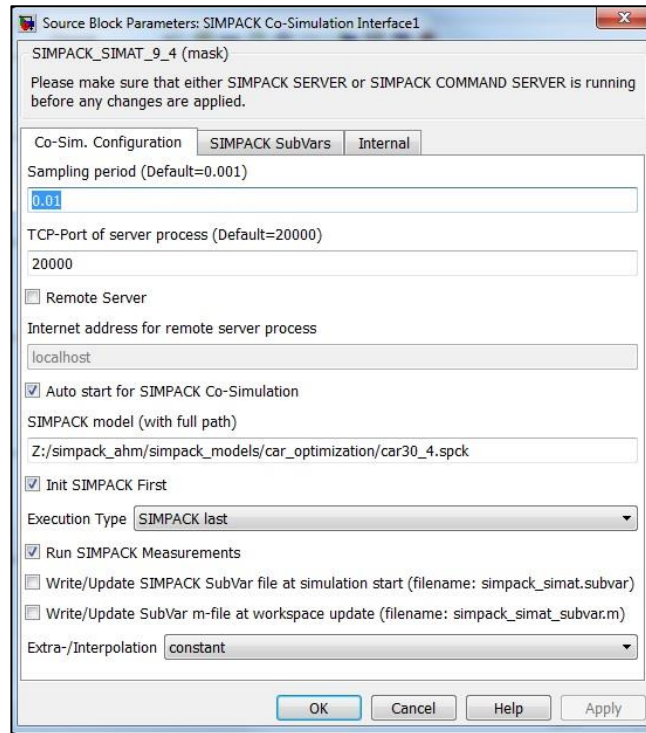


Figure 5.3 SIMAT block interface.

5.1.4 SIMPACK role

Once making use of the MATLAB – SIMPACK connection, particular parameters have to be specified in the MBS software to accomplish the assembly.

Apart from the SIMPACK “Solver Settings” panel, the simulation results that have to be sent to MATLAB must be determined by the *y-Outputs* in SIMPACK. There is no limit on the number of *y-Outputs* created but to be properly used, special attention must be paid to the sensors from which the data is acquired. Moreover, those SubVar files (which could include the values of design parameters in each iteration) modified by MATLAB must be chosen in the “SubVar File List” panel as the one from which the SIMPACK will receive the input information.

Finally, instead of clicking the button “Time Integration - Offline” used to run single simulations, the option “Co-Simulation – Start Command Server” (in reference to the tab in SIMPACK settings) must be used to complete the connection.

5.2 Genetic Algorithm method

The genetic algorithm (GA) has been applied as an optimization procedure in mechanical systems during the last thirty years [Goldber, D.E. (1989)]. Basing its working method on patterns found in the physical world, this type of algorithm is characterized by being able to find the minimum of an objective function bounded by constraints by altering design parameter values without the need of a suitable initial guess of the optimized values of design parameters.

The process executed by this algorithm consists in the codification of the set of design parameters obtained in each iteration by means of finite-length binary strings. In this way, the population of each generation (iteration) is created. To continue the process and thus building a new generation, the algorithm utilizes the following three methods founded on the fitness value, *i.e.* the value of the objective function under study [Baumal, A.E., McPhee, J.J. and Calamai, P.H. (1996)].

1. **Reproduction.** The creation of a new generation is based on a pair of already created generation. Thus, the new one shares the attributes that define the parents.

2. **Crossover.** This technique is used to create a new generation by exchanging strings amongst several randomly chosen pairs of generations.

3. **Mutation.** In this last case the creation of new generations is carried out by the modification of one or more strings of a previously created generation.

By the use of one or more of these methods, the algorithm searches for the best solution through an iterative procedure. When dealing with multiobjective optimization problems, the creation of the Pareto-front is normally used.

The characteristics defining the GA used in all the optimizations are summarized in Table 5.1.

Table 5.1 Optimization algorithm settings.

Population size	40
Tolerance in fitness value (TolFun)	$1 \cdot 10^{-4}$
Maximum number of generations	841

Finally, the stopping criterion for every optimization performed in this project is the convergence of the optimization problem or the achievement of the maximum number of generations.

5.3 Rail–wheel wear optimization

The first part concerning the optimization of the primary passive suspension of the railway model is focused on the optimization of the rail-wheel wear objective function. The reason of this selection among the three previously defined objective functions is that the maximum rate of wear at the contact point between rail and wheel has been subject to severe restrictions in the last few years in order to reduce maintenance costs in both rails and wheels. Moreover, a lower wear rate means higher travelling velocity on small radius curves and improved dynamic behaviour which is closely related to safety against derailment.

5.3.1 Wear optimization with longitudinal and lateral primary stiffness as design parameters

According to [Suarez B., Mera J.M., Martinez M.L. and Chover J.A. (2012)] the elastic elements belonging to the primary suspension of a railway vehicle with the highest influence on the rail-wheel wear are the longitudinal and lateral springs. Based on this study, the minimization of wear objective function is performed with respect to the two above mentioned elements maintaining the stiffness value in the vertical direction equal to a proper constant value. Thus, the computation time is reduced in comparison with the case in which the elastic elements in the three directions are considered.

The definition of the optimization problem of one objective function can be formulated as follows: given wear objective function $\Gamma_W(k_X^p, k_Y^p)$ governed by the primary longitudinal and lateral stiffness as design parameters, it is required to determine the optimal value of the design parameters which satisfy the equation (5.1).

$$\Gamma_W(k_{X,opt}^p, k_{Y,opt}^p) = \min_{k_X, k_Y \in \mathcal{X}} \Gamma_W(k_X^p, k_Y^p) \quad (5.1)$$

Where \mathcal{X} represents the design variables boundaries and the thresholds of the problem are the two remaining objective functions, comfort and safety, which must satisfy the standards.

To finalize the definition of this optimization problem the initial value of the design parameters as well as their boundaries are given in Table 5.2.

Table 5.2 *Design parameters boundaries and initial value in $\Gamma_{WEAR}(k_X, k_Y)$ optimization.*

Design parameter	Lower bound (N/m)	Upper bound (N/m)	Initial value (N/m)
k_X^p	0	10^8	$6.9 \cdot 10^6$
k_Y^p	0	10^8	$0.9 \cdot 10^6$

From this first optimization with respect to wear objective function, Figure 5.4 summarizes the results.

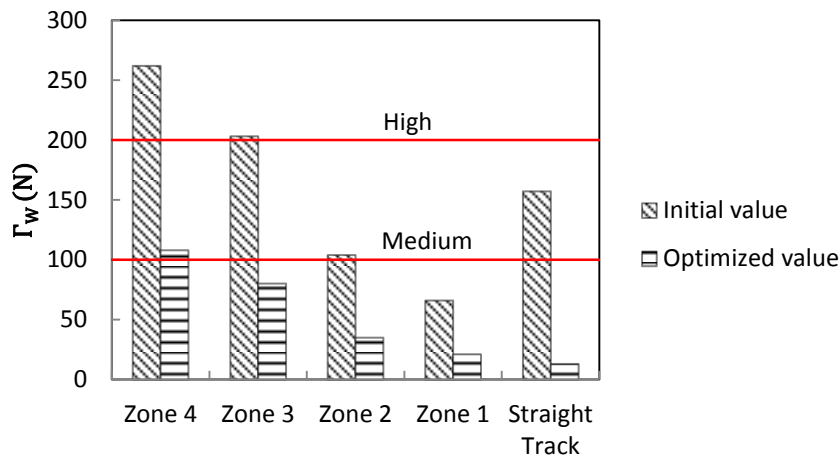


Figure 5.4 Results from $\Gamma_{WEAR}(k_X, k_Y)$ optimization in every scenario.

Table 5.3 summarizes the optimized results illustrated in Figure 5.4.

Table 5.3 Wear optimized values for each operational scenario in $\Gamma_{WEAR}(k_X, k_Y)$.

Obj. Function	Zone 4	Zone 3	Zone 2	Zone 1	Tangent
$\Gamma_W(N)$	108	80	35	21	13

From Figure 5.4, it can be stated that the value of wear objective function is reduced in every operational scenario due to the optimization performed demonstrating that the longitudinal and lateral primary stiffness have a strong effect on the performances of a railway vehicle. In this way, the level of “High Wear” is no longer achieved for any case and in particular, a strong reduction close to 90% of the initial value has been achieved for “Straight Track” operational scenario. The reason that could explain this situation is that the initial suspension parameters were defined as an equilibrium solution in order to have acceptable vehicle dynamic behaviour in every type of scenario.

In Figure 5.5 the initial and optimized values of the longitudinal primary stiffness design parameters are given.

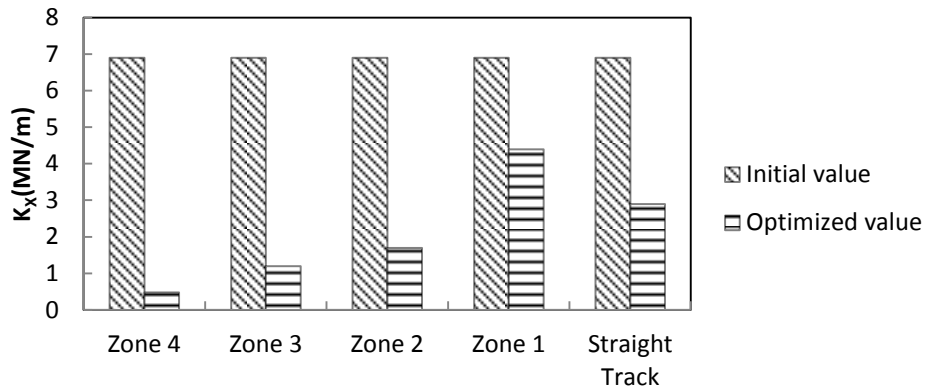


Figure 5.5 Longitudinal primary stiffness value in $\Gamma_{WEAR}(k_X, k_Y)$.

Table 5.4 summarizes the optimized results illustrated in Figure 5.5.

Table 5.4 Optimized longitudinal stiffness for each operational scenario in $\Gamma_{WEAR}(k_X, k_Y)$.

Parameter	Zone 4	Zone 3	Zone 2	Zone 1	Tangent
k_X (MN/m)	0.48	1.2	1.7	4.4	2.9

Figure 5.5 demonstrates that the primary longitudinal stiffness value needed to obtain the best performances in every operational scenario is considerably smaller than the initial value. The biggest reduction occurs in the three curved track scenarios with smallest radius of curvature and it can be due to the fact that smaller values of primary longitudinal stiffness enhance the ability of the wheelsets to rotate with respect to the bogie frame and thus improving their behaviour when entering in a curve.

Figure 5.6 shows the initial and optimized values of the lateral primary stiffness design parameter.

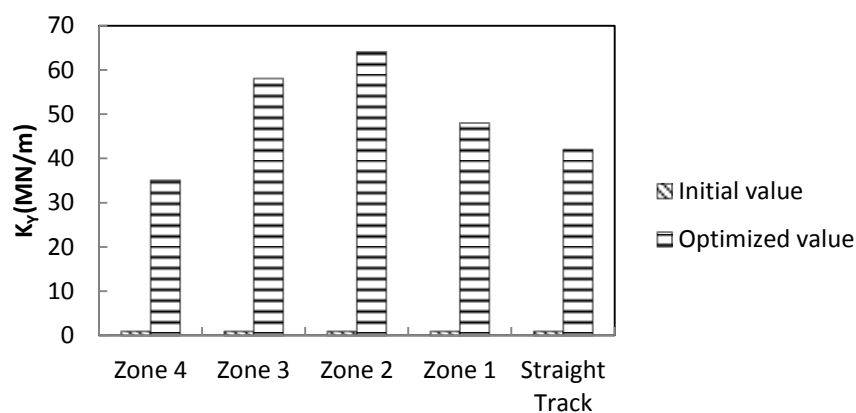


Figure 5.6 Lateral primary stiffness value in $\Gamma_{WEAR}(k_X, k_Y)$.

Table 5.5 summarizes the optimized results illustrated in Figure 5.6.

Table 5.5 Optimized lateral stiffness for each operational scenario in $\Gamma_{WEAR}(k_X, k_Y)$.

Parameter	Zone 4	Zone 3	Zone 2	Zone 1	Tangent
$k_Y(MN/m)$	35	58	64	48	42

As Figure 5.6 displays, this first optimization with respect to wear objective function leads to a significant change on the value of the lateral primary stiffness. From the initial value equal to $0.9MN/m$ for each operational scenario, the optimized values are bigger than one order of magnitude with respect to the initial one. This difference can be due to the fact that a bigger value of lateral primary stiffness reduces the relative movement of the wheelsets with respect to the bogie frame in the lateral direction and as a consequence, the frequency and severity of the contact between wheel flange and rail is reduced and thus the wear is minimized.

As it has been previously specified, the other two objective functions must satisfy the limits given by the standards when using the results obtained from the optimization. Figure 5.7 and Figure 5.8 resume the initial and optimized values of safety objective functions for this optimization problem. Moreover Table 5.3 displays the initial and optimized values of comfort objective functions.

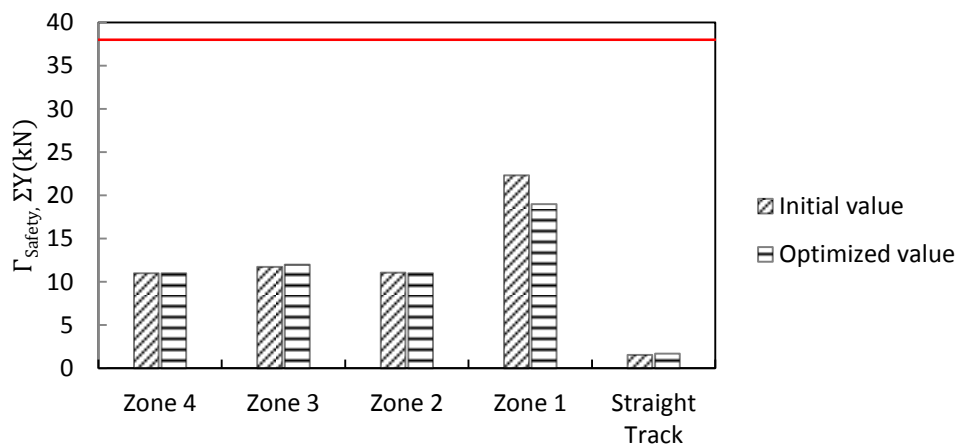


Figure 5.7 Track shift force values in $\Gamma_{WEAR}(k_X, k_Y)$.

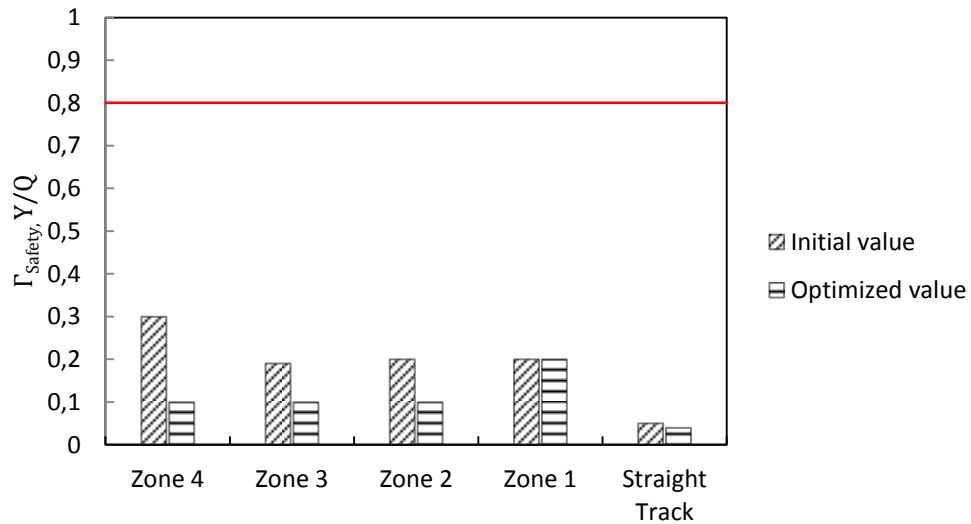


Figure 5.8 Derailment coefficient values in $\Gamma_{WEAR}(k_X, k_Y)$.

Table 5.6 Comfort values in $\Gamma_{WEAR}(k_X, k_Y)$.

	Zone 4		Zone 3		Zone 2		Zone 1		Tangent	
	I	O	I	O	I	O	I	O	I	O
Front	0.7	2.1	1.2	2.0	1.2	1.9	3.0	2.2	3.5	1.9
Centre	0.4	1.4	0.7	1.1	0.8	1.0	1.6	1.4	2.2	1.4
Rear	0.5	2.0	1.0	1.8	1.0	1.5	2.6	2.0	3.8	2.4

Note that in Table 5.6, I and O stand for “Initial” and “Optimized” respectively and the first column makes reference to the different points in which the comfort is evaluated.

5.3.2 Wear optimization with respect to the primary damping coefficients

For the second wear objective function optimization, the primary passive dampers on the three directions (longitudinal, lateral and vertical) are selected as design parameters. Moreover, the values of the longitudinal and lateral primary passive stiffness are equal to the optimized values achieved from the previous optimization.

In this case, the definition of the optimization problem is formulated as follows: given the wear objective function $\Gamma_{\text{Wear}}(c_X^p, c_Y^p, c_Z^p)$ governed by the primary longitudinal, lateral and vertical damping coefficients as design parameters, it is required to determine the optimal values of the design parameters which satisfy the equation (5.2).

$$\Gamma_W(c_{X,opt}^p, c_{Y,opt}^p, c_{Z,opt}^p) = \min_{c_X, c_Y, c_Z \in \mathcal{X}} \Gamma_W(c_X^p, c_Y^p, c_Z^p) \quad (5.2)$$

Where \mathcal{X} represents the design variables boundaries. Moreover, the thresholds are the two remaining objective functions (i.e. ride comfort and safety) which must satisfy the limits imposed by the standards.

To finalize the definition of this optimization problem the initial value of the design parameters as well as their boundaries are given in Table 5.7.

Table 5.7 Design parameters boundaries and initial values in $\Gamma_{\text{WEAR}}(c_X^p, c_Y^p, c_Z^p)$ optimization.

Design parameter	Lower bound (Ns/m)	Upper bound (Ns/m)	Initial value (Ns/m)
c_X^p	0	10^6	$0.1 \cdot 10^3$
c_Y^p	0	10^6	$35 \cdot 10^3$
c_Z^p	0	10^6	$35 \cdot 10^3$

The results obtained from this second optimization with respect to wear objective function are summarized in Figure 5.9.

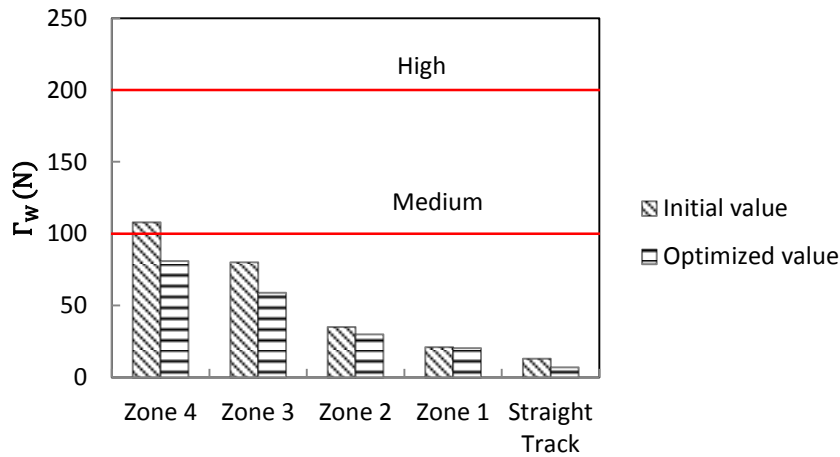


Figure 5.9 Results from $\Gamma_{WEAR}(c^P_X, c^P_Y, c^P_Z)$ optimization in every scenario.

Table 5.8 summarizes the optimized results illustrated in Figure 5.9.

Table 5.8 Wear optimized values for each operational scenario in $\Gamma_{WEAR}(c^P_X, c^P_Y, c^P_Z)$.

Obj. Function	Zone 4	Zone 3	Zone 2	Zone 1	Tangent
$\Gamma_w(N)$	81	59	30	20.5	7

As it can be seen in Figure 5.9, the optimization of wear objective function with respect to the primary dampers has a smaller effect in comparison to the case in which the stiffness are considered as design parameters. Nonetheless, an improvement of the wear value is achieved leading to the situation in which the value of the objective function falls for every operational scenario inside the category of “Low” wear value.

In Figure 5.10 the initial and optimized values of the longitudinal primary damping coefficient design parameter are given.

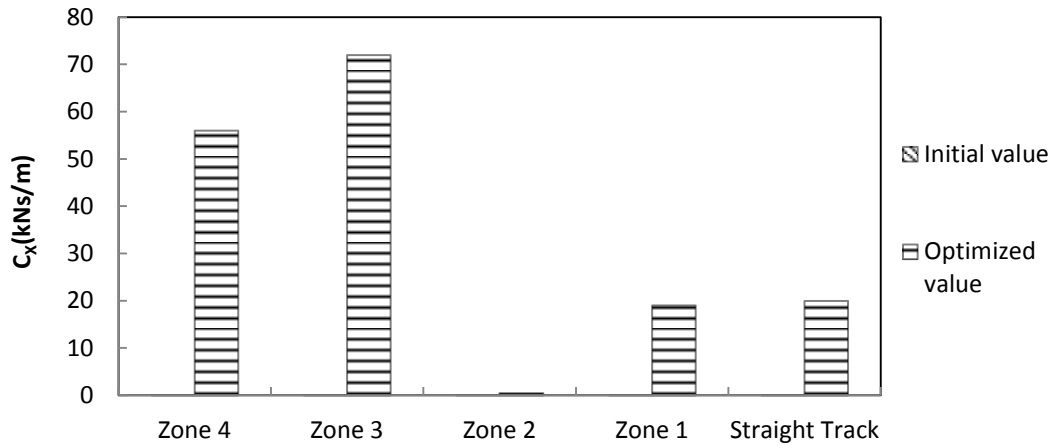


Figure 5.10 Longitudinal primary damping coefficient value in $\Gamma_{WEAR}(c_X^P, c_Y^P, c_Z^P)$.

Table 5.9 summarizes the optimized results illustrated in Figure 5.10.

Table 5.9 Optimized longitudinal damping coefficient for each operational scenario in $\Gamma_{WEAR}(c_X^P, c_Y^P, c_Z^P)$.

Parameter	Zone 4	Zone 3	Zone 2	Zone 1	Tangent
$c_X(kNs/m)$	56	72	0.45	19	20

Note that every value is represented, but due to the high difference between them, only the biggest appear.

As it can be seen in Figure 5.10, the optimized values of the longitudinal primary damping coefficient are considerably much higher than the initial ones. The main increments correspond to “Zone4-Very small radius curve” and “Zone3-Small radius curve” operational scenarios. It is in these two operational scenarios where the wheelsets yaw angle achieves the highest values and by means of a high value of longitudinal damping coefficient this rotational movement is performed in a more stable way.

Figure 5.11 shows the initial and optimized values of the lateral primary damping coefficient design parameter.

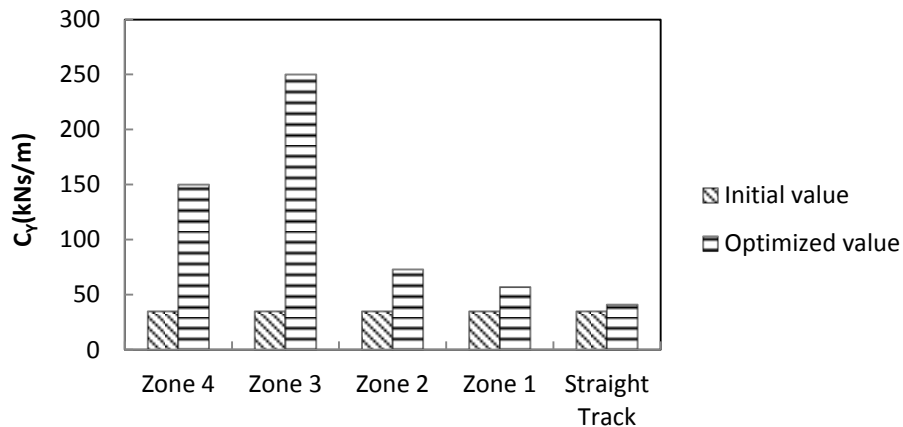


Figure 5.11 Lateral primary damping coefficient value in $\Gamma_{WEAR}(c^P_X, c^P_Y, c^P_Z)$.

Table 5.10 summarizes the optimized results illustrated in Figure 5.11.

Table 5.10 Optimized lateral damping coefficient for each operational scenario in $\Gamma_{WEAR}(c^P_X, c^P_Y, c^P_Z)$.

Parameter	Zone 4	Zone 3	Zone 2	Zone 1	Tangent
$c_Y(kNs/m)$	150	250	73	57	41

For the case of the lateral primary damping coefficient values, the optimized ones are slightly bigger than the initial values. The biggest difference is found in “Zone4-Very small radius curve” and “Zone3-Small radius curve” operational scenarios and it may respond to the need of reducing the lateral relative displacement between wheelsets and bogie frame minimizing the flange contact and thus reducing the wear rate.

Figure 5.12 shows the initial and optimized values of the vertical primary damping coefficient design parameter. As well as for the case of the lateral primary damping coefficient, the optimized values are similar to the initial ones except for the case of “Straight Track” operational scenario, in which the optimized value is considerably bigger than the initial one. The reason of such situation may be that the high value of speed at which the railway model travels in that operational scenario provokes significant level of vibrations in the vertical direction, causing a more irregular contact between wheel and rail. And a possible way to solve this situation is increasing the value of the damping coefficient in the vertical direction.

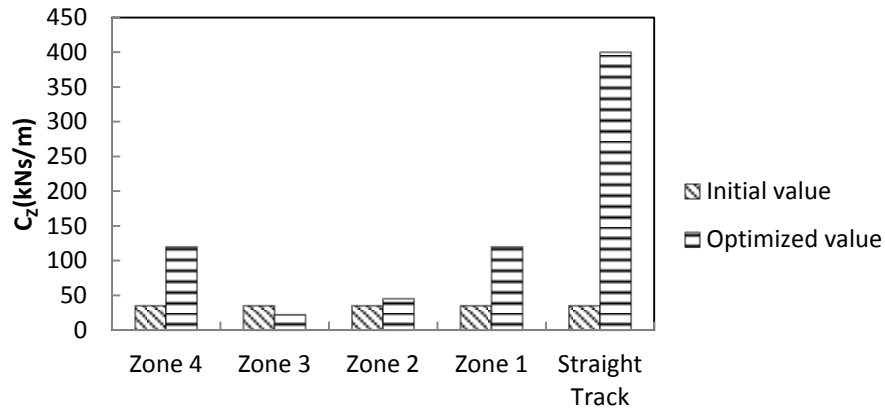


Figure 5.12 Vertical primary damping coefficient value in $\Gamma_{WEAR}(c^P_X, c^P_Y, c^P_Z)$.

Table 5.11 summarizes the optimized results illustrated in Figure 5.12.

Table 5.11 Optimized lateral damping coefficient for each operational scenario in $\Gamma_{WEAR}(c^P_X, c^P_Y, c^P_Z)$.

Parameter	Zone 4	Zone 3	Zone 2	Zone 1	Tangent
$c_Z(kNs/m)$	120	22	45	120	400

With respect to the values of safety objective function, Figures 5.13 and 5.14 illustrate the initial and optimized values, demonstrating that in every case the limits defined by standards are respected.

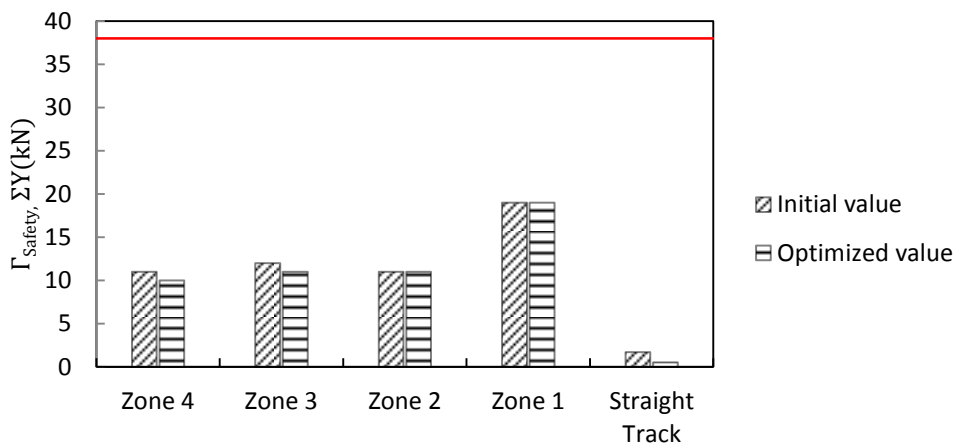


Figure 5.13 Track shift force values in $\Gamma_{WEAR}(c^P_X, c^P_Y, c^P_Z)$.

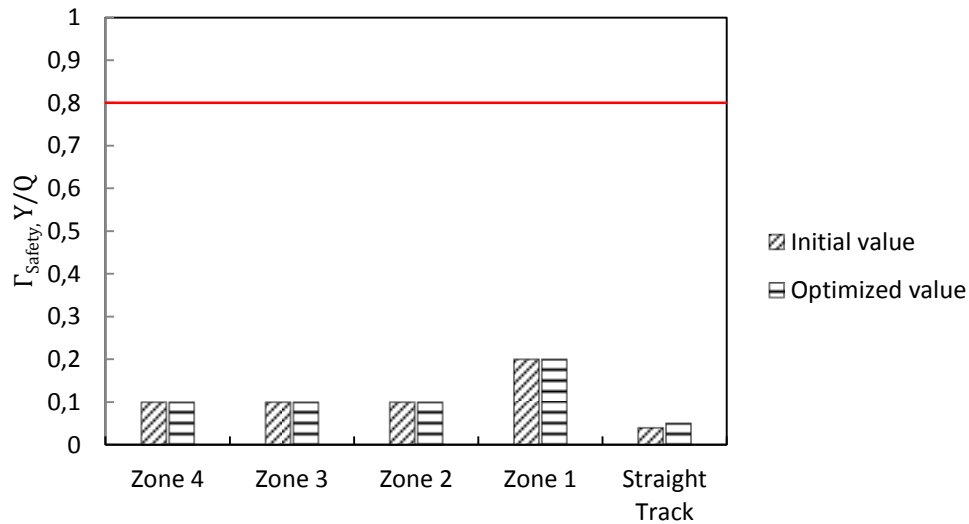


Figure 5.14 Derailment coefficient values in $\Gamma_{WEAR}(c^P_X, c^P_Y, c^P_Z)$.

With respect to comfort objective function, Table 5.12 shows the initial and optimized values.

Table 5.12 Comfort values in $\Gamma_{WEAR}(c^P_X, c^P_Y, c^P_Z)$.

	Zone 4		Zone 3		Zone 2		Zone 1		Tangent	
	I	O	I	O	I	O	I	O	I	O
Front	2.1	1.6	2.0	1.9	1.9	2	2.2	2.2	1.9	2
Centre	1.4	0.9	1.1	1.0	1.0	1.0	1.4	1.3	1.4	1.3
Rear	2.0	1.4	1.8	1.7	1.5	1.5	2.0	2	2.4	2.3

Note that in Table 5.12, I and O stand for “Initial” and “Optimized” respectively and the first column makes reference to the different points in which the comfort is evaluated.

5.4 Rail–wheel wear and ride comfort optimization

The second sets of optimizations are focused on the minimization of wheel-rail wear and ride comfort objective functions while having safety as a threshold. The reason why ride comfort is included in the optimizations as a second objective function is because it is the main parameter that can be felt by the passengers in a railway operation once safety issues are ensured.

As stated in chapter 2 and in particular section 2.1.2, according to [CEN (1999)] ride comfort has to be measured in three points along the railway vehicle. But in order to deal with a bi-objective optimization problem (with wheel-rail wear and ride comfort as objective functions), a new parameter containing the contribution of those three points is defined according to equation (5.3):

$$\Gamma_C = \sqrt{(N_{MV}^F)^2 + (N_{MV}^C)^2 + (N_{MV}^R)^2} \quad (5.3)$$

Where N_{MV}^F , N_{MV}^C and N_{MV}^R stand for the value of ride comfort at the front, center and rear point of the railway vehicle model, respectively. This new function together with wear objective function should be minimized during the new optimization problems.

5.4.1 Rail–wheel wear and ride comfort optimization with longitudinal and lateral primary stiffness as design parameters

Following the same procedure explained in Section 5.3, this optimization is characterized by having the primary longitudinal and lateral stiffness as design parameters according to [Suarez B., Mera J.M., Martinez M.L. and Chover J.A. (2012)]. It should be noted that, the value of the vertical primary stiffness is maintained constant and only the value of safety is used as a threshold.

The mathematical representation of the bi-objective optimization problem is formulated as follows: given the vector of objective functions $F(k_X^p, k_Y^p) = [\Gamma_W, \Gamma_C]$ governed by the primary longitudinal and lateral stiffness as design parameters, it is required to determine the optimal values of the design parameters which satisfy the equations (5.4) and (5.5).

$$\Gamma_W(k_{X,opt}^p, k_{Y,opt}^p) = \min_{k_X, k_Y \in \mathcal{X}} \Gamma_W(k_X^p, k_Y^p) \quad (5.4)$$

$$\Gamma_C(k_{X,opt}^p, k_{Y,opt}^p) = \min_{k_X, k_Y \in \mathcal{X}} \Gamma_C(k_X^p, k_Y^p) \quad (5.5)$$

Where \mathcal{X} represents the design variables boundaries and the problem threshold is safety objective function which must satisfy the limits imposed by the standards.

To finalize the definition of this optimization problem the boundaries of the design parameters are given in Table 5.2. Must be noted that the initial values of the design parameters are equal to the optimized values resulting from the optimization problem discussed in Section 5.3.1. Moreover, the values of the damping coefficients used are the ones obtained from the optimization explained in Section 5.3.2. This is done in order to take advantage of the results already achieved.

From the fact that this optimization problem deals with two objective functions simultaneously, the results are shown as a Pareto front which is the accepted way of showing multi-objective optimization results. The points that form such line are the different solutions for the optimization problem.

For the case of “Zone4–Very small radius curve” operational scenario, the Pareto front in which the possible solutions are presented can be seen in Figure 5.15.

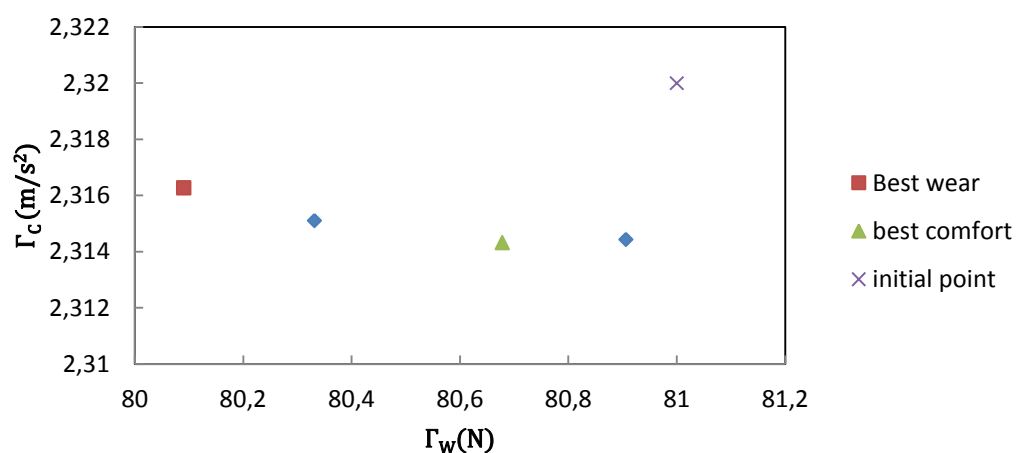


Figure 5.15 Pareto-front for Zone4 scenario in $F(k_X, k_Y)$ problem.

Figure 5.15 demonstrates that the capacity of improving the values of both objective functions by means of a third optimization is limited. This is so not only because the situation obtained at the end of the previous optimization problem is considered as starting point but also because a second objective function is taken into account. Nevertheless, four combinations of design parameters are found leading to improvements in both wear and comfort objective functions.

The values of the design parameters corresponding to the points appearing in the previous graph are represented as the Pareto-sets in Figure 5.16. It can be seen that the case with the best wear value corresponds to a small increment of both longitudinal and lateral primary stiffness and more interesting, the case with the best comfort value is achieved by an increment of the longitudinal primary stiffness which may lead to a reduction of the accelerations transmitted to the bogie frame.

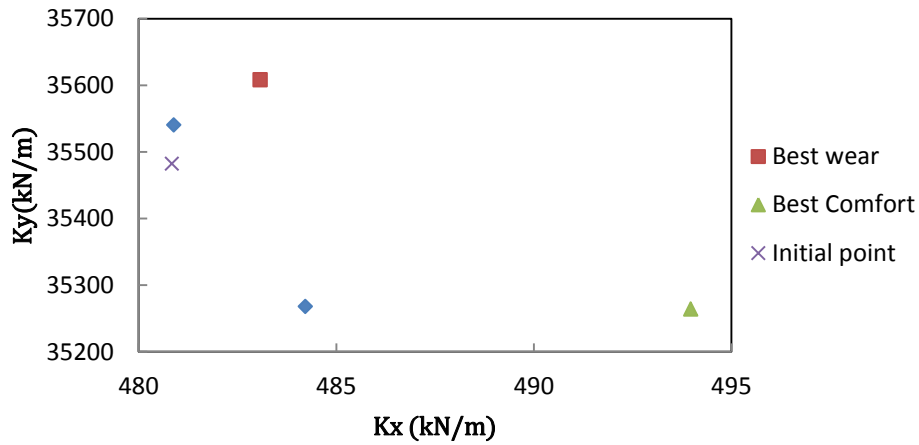


Figure 5.16 Pareto-sets for Zone4 scenario in $F(k_x, k_y)$ problem.

For the case of “Zone3-Small radius curve” scenario, Figure 5.17 represents the resulting graph achieved from the optimization.

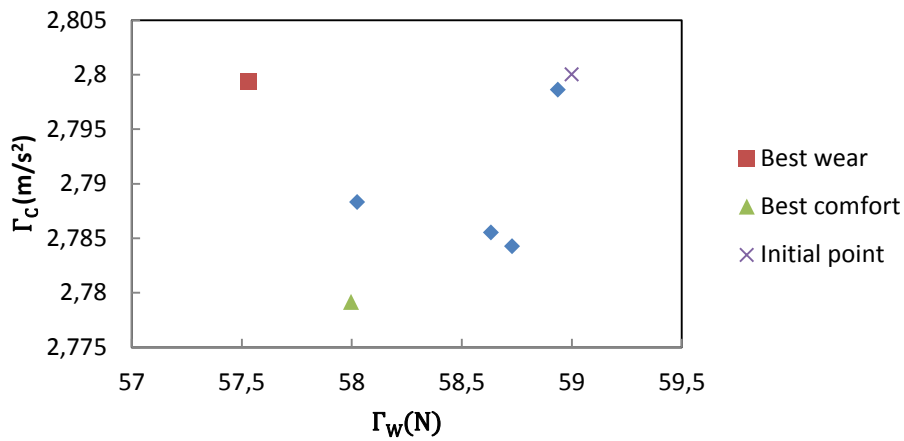


Figure 5.17 Pareto-front for Zone3 scenario in $F(k_x, k_y)$ problem.

For the case of this operational scenario, the optimization results show six combinations of the design parameters which are probed to give an improvement in the objective functions value. Even if the advance can be considered small, the biggest achievement from this optimization may be the fact that the wear value has been decreased in one point.

The values of the design parameters corresponding to the points appearing in the previous graph are represented as the Pareto-sets in Figure 5.18. It may be clear that the case with the best wear value is characterized by a significant increase of the lateral primary stiffness with respect to the initial case. This may respond to a reduction of the wheel flange contact. The case with the best comfort value is characterized by an increment of both longitudinal and lateral stiffness with respect to the initial case, and may respond to an effort in increasing the general stiffness of the system to reduce the accelerations transmitted to the bogie frame.

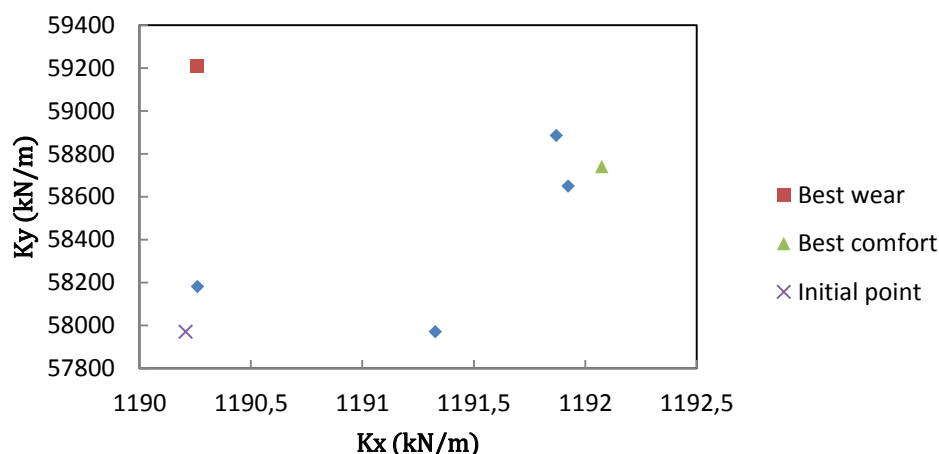


Figure 5.18 Pareto-sets for Zone3 scenario in $F(k_x, k_y)$ problem

For the case of “Zone2 – Medium radius curve” scenario, Figure 5.19 represents the resulting graph achieved from in the optimization.

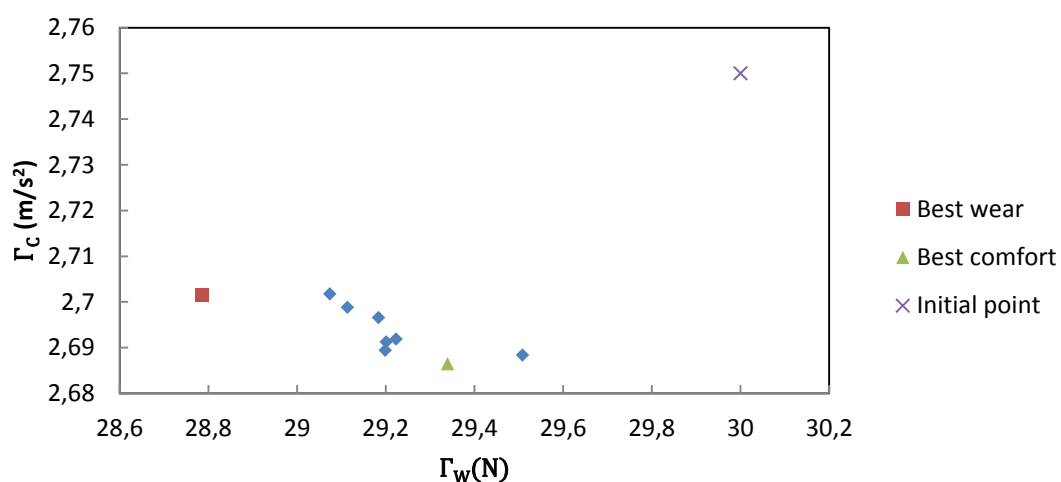


Figure 5.19 Pareto-front for Zone2 scenario in $F(k_x, k_y)$ problem.

For this particular scenario, the optimization results are composed by nine points forming the Pareto front. Moreover, the improvement obtained in this optimization is reflected in better value of both objective functions.

The values of the design parameters corresponding to the points appearing in the previous graph are represented in Figure 5.20. As it can be seen, there is a considerable difference in terms of both stiffness values between the initial case and the ones forming the Pareto front.

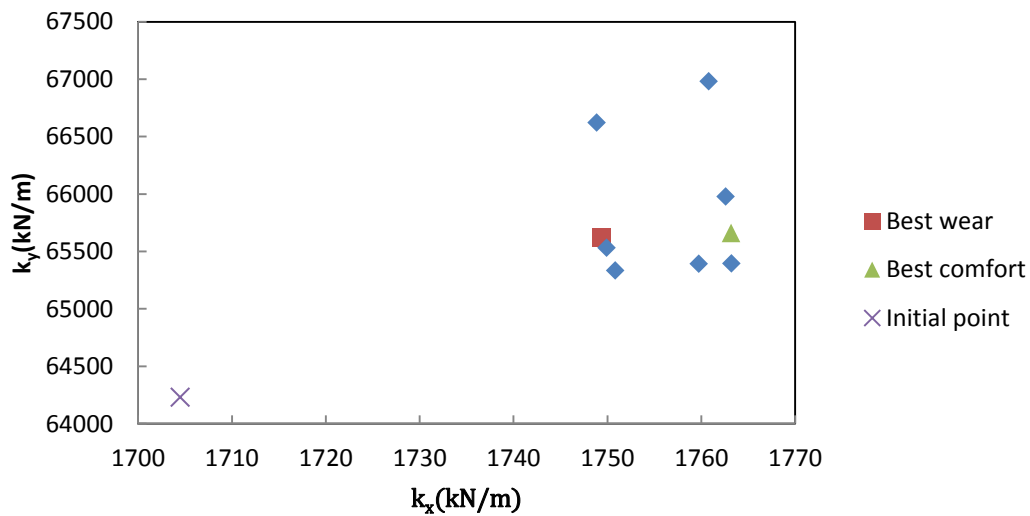


Figure 5.20 Pareto-sets for Zone2 scenario in $F(k_x, k_y)$ problem

For the case of “Zone1-Large radius curve” scenario, Figure 5.21 represents the resulting graph achieved from the optimization. In this particular scenario, the Pareto front reveals that five different combinations of the design parameters lead to better values of the objective functions. In particular, this optimization shows that a quite significant improvement of the wear value can be achieved while reducing very slightly the comfort value.

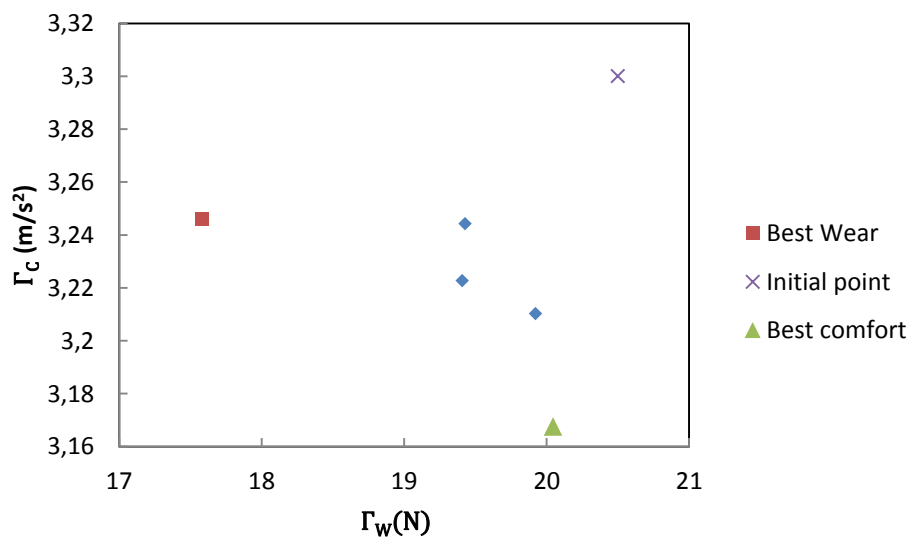


Figure 5.21 Pareto-front for Zone1 scenario in $F(k_x, k_y)$ problem.

The values of the design parameters corresponding to the points appearing in the previous graph are represented as the Pareto-front in Figure 5.22. This figure demonstrates that in order to obtain the enhancements previously mentioned, it is necessary to reduce both longitudinal and lateral stiffness.

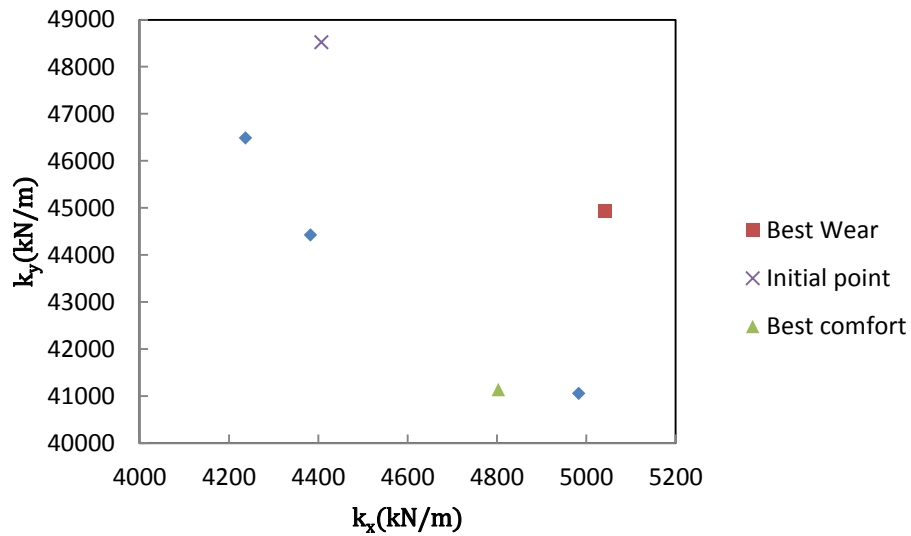


Figure 5.22 Pareto-sets for Zone1 scenario in $F(k_x, k_y)$ problem.

For the case of “Straight Track” scenario, Figure 5.23 represents the resulting graph achieved from in the optimization. For this final case, the optimization solution shows the possibility of improvement through seven points forming the Pareto graph which are characterized at the same time by better values of wear and comfort.

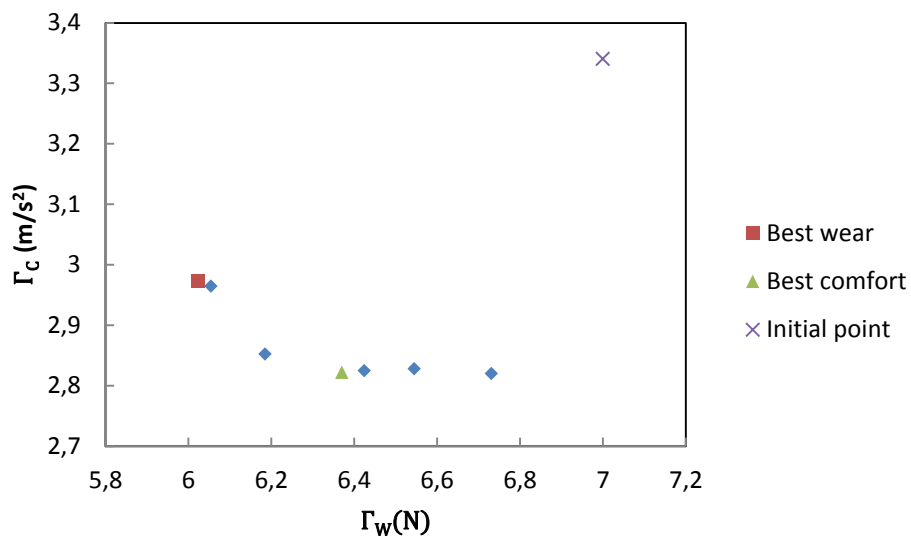


Figure 5.23 Pareto-front for Straight Track scenario in $F(k_x, k_y)$ problem.

The values of the design parameters corresponding to the points appearing in the previous graph are represented in Figure 5.24.

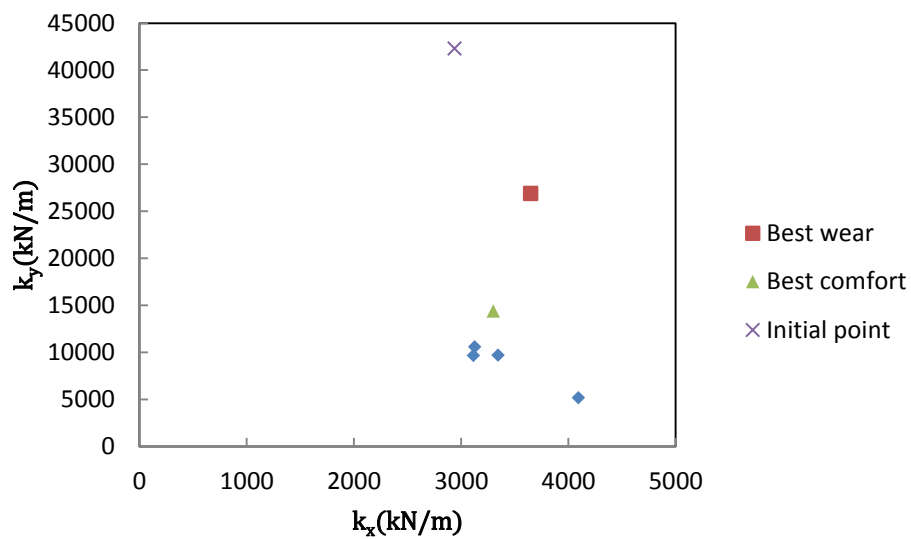


Figure 5.24 Pareto-sets for Straight Track scenario in $F(k_x, k_y)$ problem

Finally, Figures 5.25 and 5.26 and show the value of safety objective function for the five operational scenarios after this optimization, demonstrating that the limits specified by the standards are satisfied.

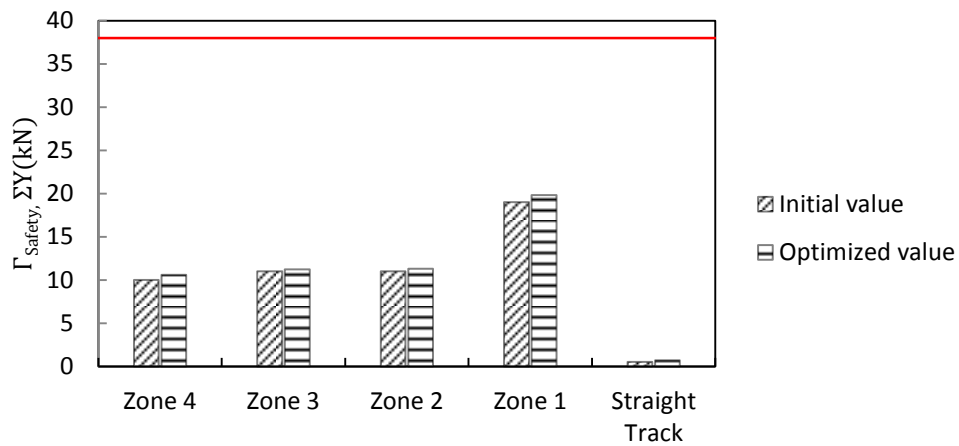


Figure 5.25 Track shift force values in $F(k_x, k_y)$.

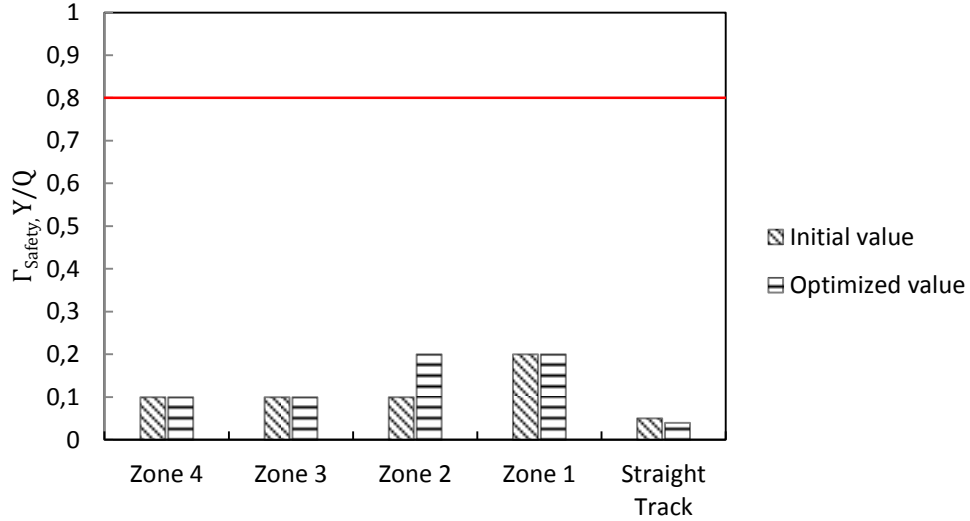


Figure 5.26 Derailment coefficient values in $F(k_X, k_Y)$.

5.4.2 Wear and ride comfort optimization with primary dampers as design parameters

For the second optimization problem in which the wear and comfort objective functions are considered, the primary passive dampers on the three directions are selected as the design parameters. Moreover and as done in the previous cases, the values of the longitudinal and lateral primary passive stiffness are equal to the optimized values achieved in the optimization problem explained in Section 5.4.1.

In this case, the definition of the optimization problem is formulated as follows. Having the vector of objective functions $F(c_X^p, c_Y^p, c_Z^p) = [\Gamma_W, \Gamma_C]$ governed by the primary longitudinal, lateral and vertical damping coefficients as design parameters, it is required to determine the optimal value of the design parameters which satisfy the equations (5.6) and (5.7).

$$\Gamma_W(c_{X,opt}^p, c_{Y,opt}^p, c_{Z,opt}^p) = \min_{c_X, c_Y, c_Z \in \mathcal{X}} \Gamma_W(c_X^p, c_Y^p, c_Z^p) \quad (5.6)$$

$$\Gamma_C(c_{X,opt}^p, c_{Y,opt}^p, c_{Z,opt}^p) = \min_{c_X, c_Y, c_Z \in \mathcal{X}} \Gamma_C(c_X^p, c_Y^p, c_Z^p) \quad (5.7)$$

Where \mathcal{X} represents the design variables boundaries and safety objective function is considered as the problem threshold which must satisfy the limits imposed by the standards.

To finalize the definition of this optimization problem the boundaries of the design parameters are given in Table 5.4. Moreover, the initial values of the primary damping coefficients are the optimized values obtained in Section 5.3.2.

As well as for the case explained in Section 5.3.1, this optimization problem deals with two objective functions at the same time and thus, the result will be expressed as Pareto-front and Pareto-sets graphs.

From the results obtained in this last optimization, the Pareto front for the case of “Zone4–Very small radius curve” operational scenario in which the possible solutions are presented in Figure 5.27. Once more, the optimization work is turned into a slightly improvement of both wear and comfort values. Even though this improvement may look very small, one must be considered that it corresponds to the fourth optimization.

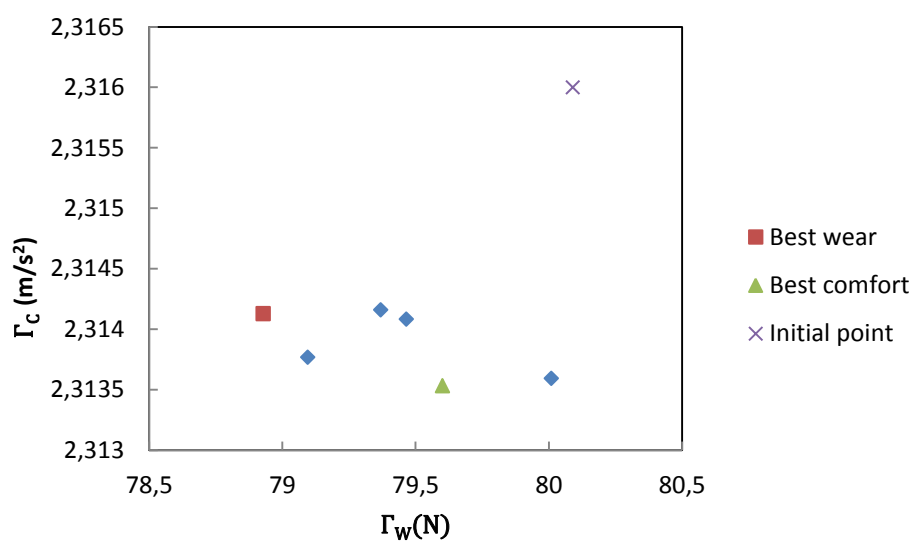


Figure 5.27 Pareto-front for Zone4 scenario in $F(c^P_x, c^P_y, c^P_z)$ problem.

The values of the design parameters corresponding to the points appearing in the previous graph are represented in Figure 5.28. As it can be seen, the variation in both design parameters is quite small (as corresponds to small improvements) and mainly in terms of the longitudinal primary damper.

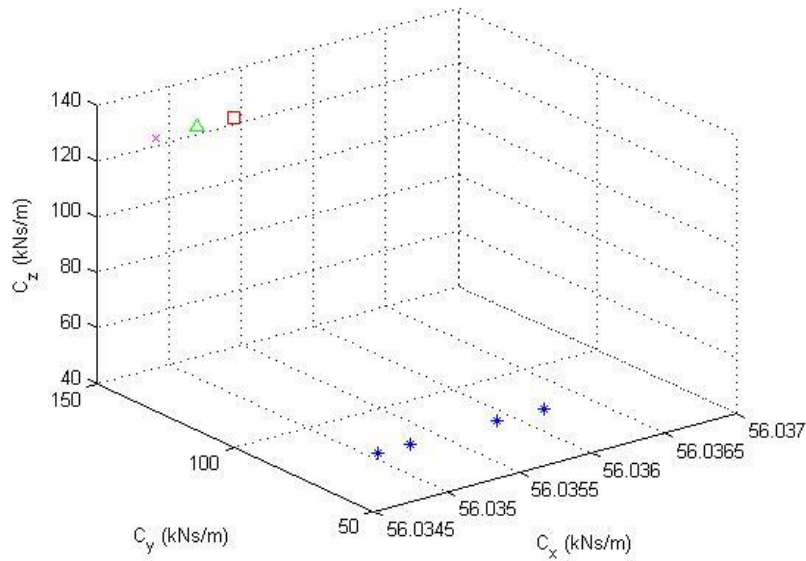


Figure 5.28 Pareto-sets for Zone4 scenario in $F(c^P_x, c^P_y, c^P_z)$ problem.

From the results obtained in this last optimization for the case of “Zone3–Small radius curve” operational scenario, the Pareto front in which the possible solutions are presented can be seen in Figure 5.29. Once more, the optimization shows that there is still possibility of a small improvement. The algorithm proposes five Pareto-sets by which both objective functions values are lightly improved.

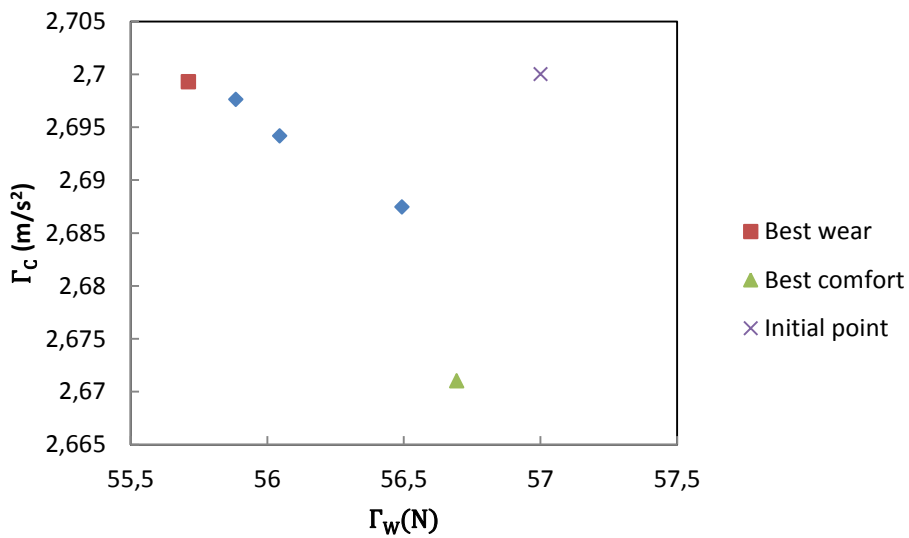


Figure 5.29 Pareto-front for Zone3 scenario in $F(c^P_x, c^P_y, c^P_z)$ problem.

The values of the design parameters corresponding to the points (Pareto-sets) appearing in the previous graph are represented in Figure 5.30. As it can be expected, the differences in terms of the design parameters values are very small among all the points appearing in the graph. But in particular, must be noted that the points forming the Pareto-front show a small reduction in the value of vertical damping coefficient as well as for the longitudinal one.

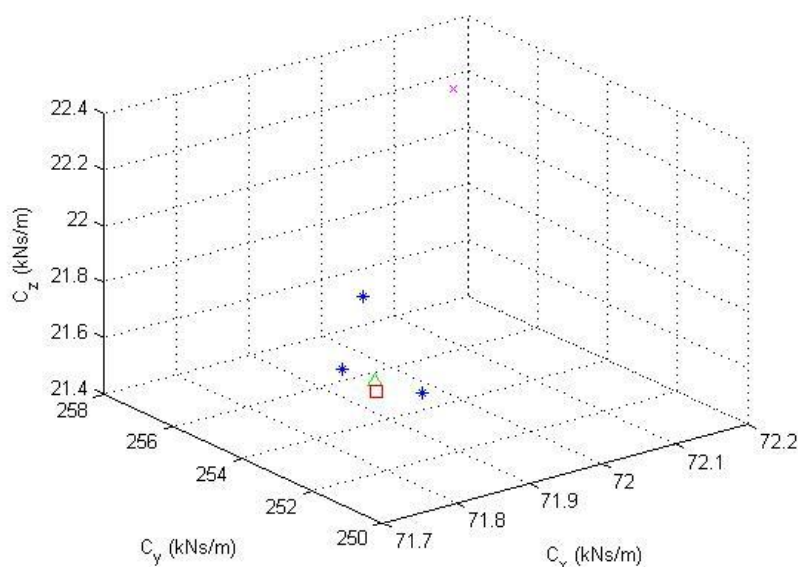


Figure 5.30 Pareto-sets for Zone3 scenario in $F(c^P_x, c^P_y, c^P_z)$ problem.

From the results obtained for the case of “Zone2-Medium radius curve” operational scenario, the Pareto-front is shown in Figure 5.31. As it can be expected, the results from a fourth optimization show a very small improvement in both wear and comfort values. Nonetheless, seven points are found as combinations of the design parameters improving the initial case.

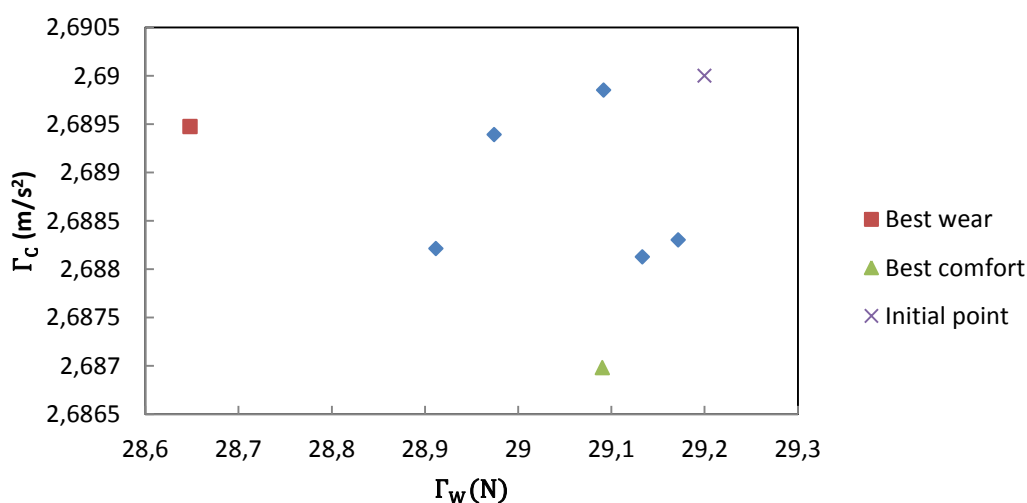


Figure 5.31 Pareto-front for Zone2 scenario in $F(c^P_x, c^P_y, c^P_z)$ problem.

The values of the design parameters (Pareto-sets) corresponding to the points appearing in the previous graph are represented in Figure 5.32. For this case, the difference between the Pareto optimal solutions and the initial case in terms of the design parameters is small.

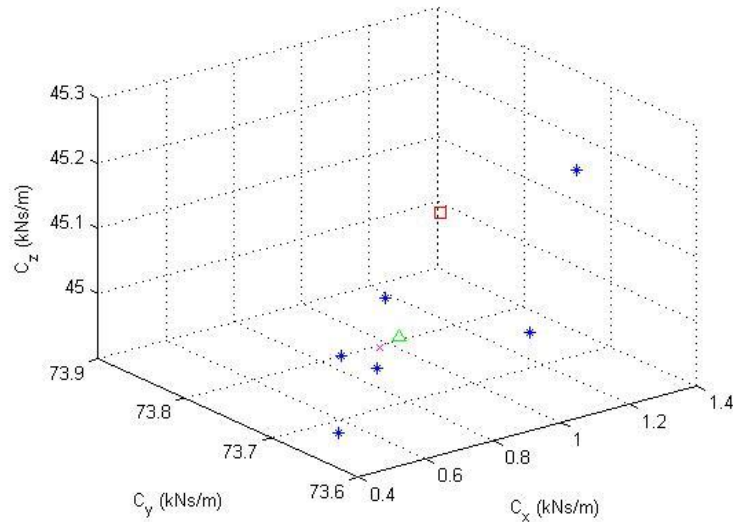


Figure 5.32 Pareto-sets for Zone2 scenario in $F(c^P_x, c^P_y, c^P_z)$ problem.

From the results obtained for the case of “Zone1-Large radius curve” operational scenario, the Pareto front in which the possible solutions are presented can be seen in Figure 5.33. For this case, only two combinations of the design parameters have been found to provide better results. Moreover and as expected from a fourth optimization the improvement is very small and could be considered as negligible.

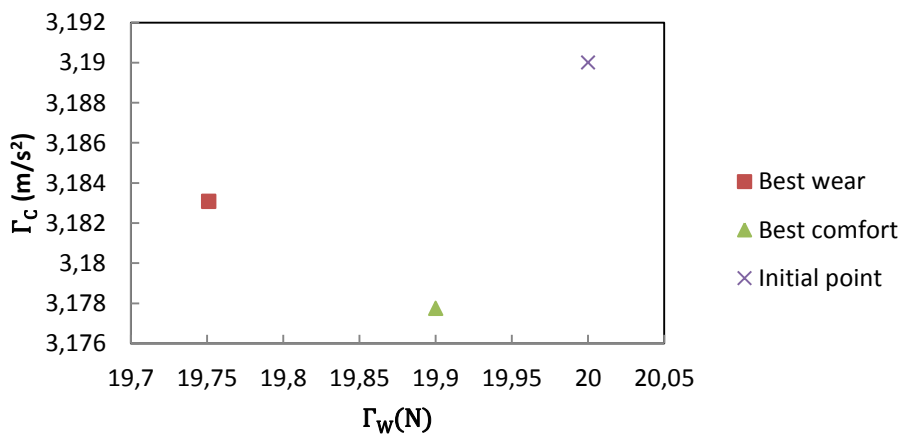


Figure 5.33 Pareto-front for Zone1 scenario in $F(c^P_x, c^P_y, c^P_z)$ problem.

The values of the design parameters (Pareto-sets) corresponding to the points appearing in the previous graph are represented in Figure 6.34. The differences in terms of the design parameters are small and as it has been said previously, their effect on the objective functions is considered very small.

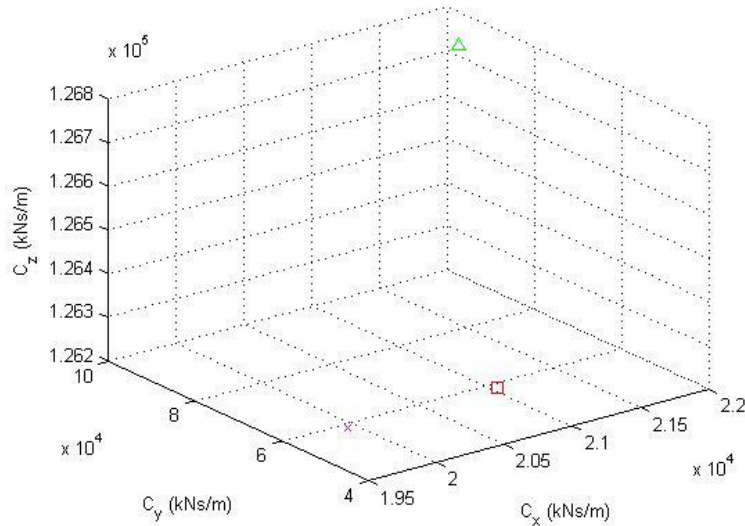


Figure 5.34 Pareto-sets for Zone1 scenario in $F(c^P_x, c^P_y, c^P_z)$ problem.

From the results obtained for the case of “Straight Track” operational scenario, the Pareto front in which the possible solutions are presented can be seen in Figure 5.35. For this last case, the results from the optimization show the existence of five different combinations of the design parameters that improve in a considerable manner the value of the objective function of the initial case.

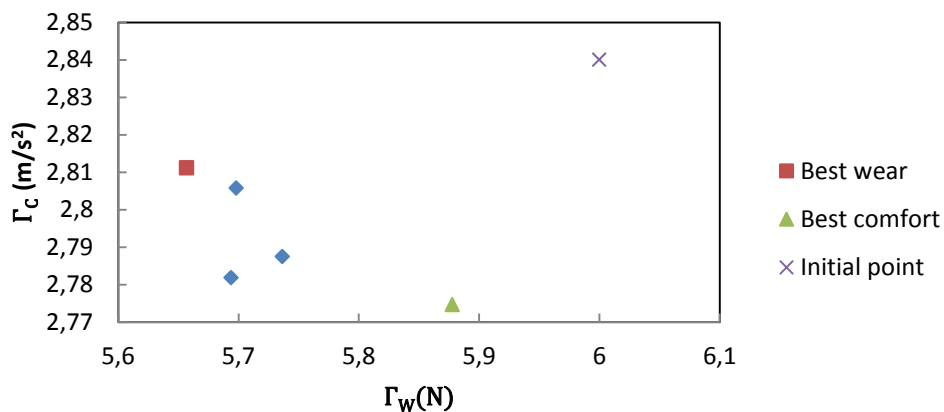


Figure 5.35 Pareto-front for Straight Track scenario in $F(c^P_x, c^P_y, c^P_z)$ problem.

The values of the design parameters (Pareto-sets) corresponding to the points appearing in the previous graph are represented in Figure 5.36. Must be said that the differences between the cases in terms of the design parameters are very small and as guessed, it is not easy to determine which element has the biggest contribution.

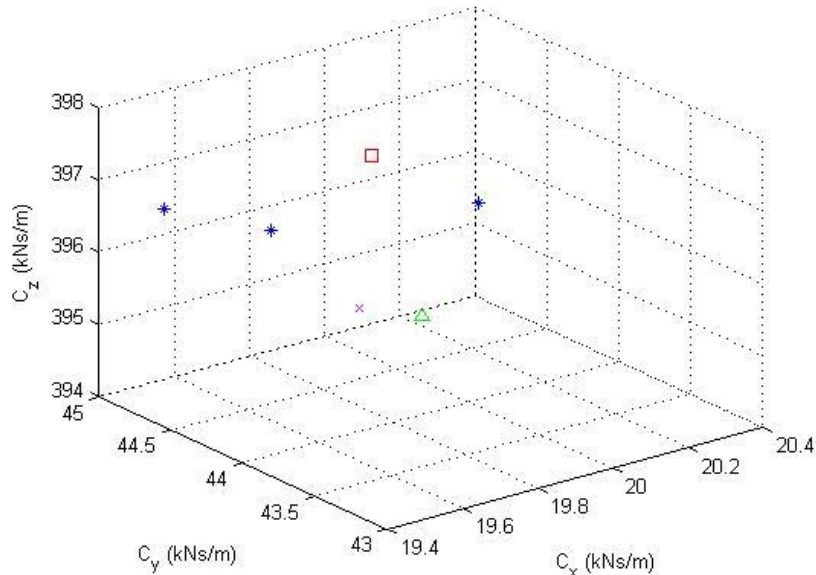


Figure 5.36 Pareto-sets for Straight Track scenario in $F(c^P_x, c^P_y, c^P_z)$ problem.

Finally, the value of the safety objective function for each case considered in this optimization are given in Figure 5.37 and Figure 5.38.

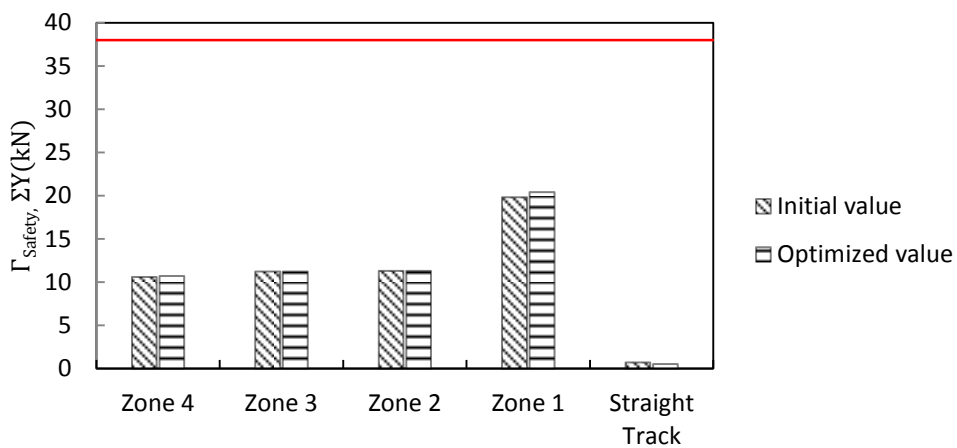


Figure 5.37 Track shift force values in $F(c^P_x, c^P_y, c^P_z)$.

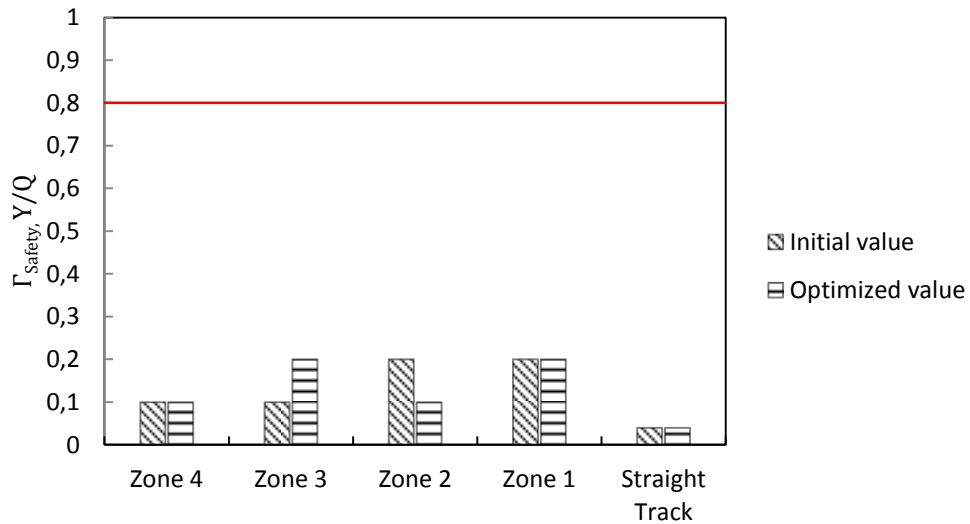


Figure 5.38 Derailment coefficient values in $F(c_X^P, c_Y^P, c_Z^P)$.

Table 5.13 represents the computation time needed for each optimization problem when using a fixed computer characterized by processor Intel® Core™ i5-660 (3.33 GHz).

Table 5.13 Computation time for each optimization.

Optimization problem	Computation time (days)
$\Gamma_{\text{Wear}}(k_X, k_Y)$	5
$\Gamma_{\text{Wear}}(c_X^P, c_Y^P, c_Z^P)$	6.5
$F(k_X^P, k_Y^P)$	7
$F(c_X^P, c_Y^P, c_Z^P)$	6.5

Finally, Figures 5.39 and 5.40 represent the results obtained through the four previously defined optimization problems for wear and comfort objective functions, respectively.

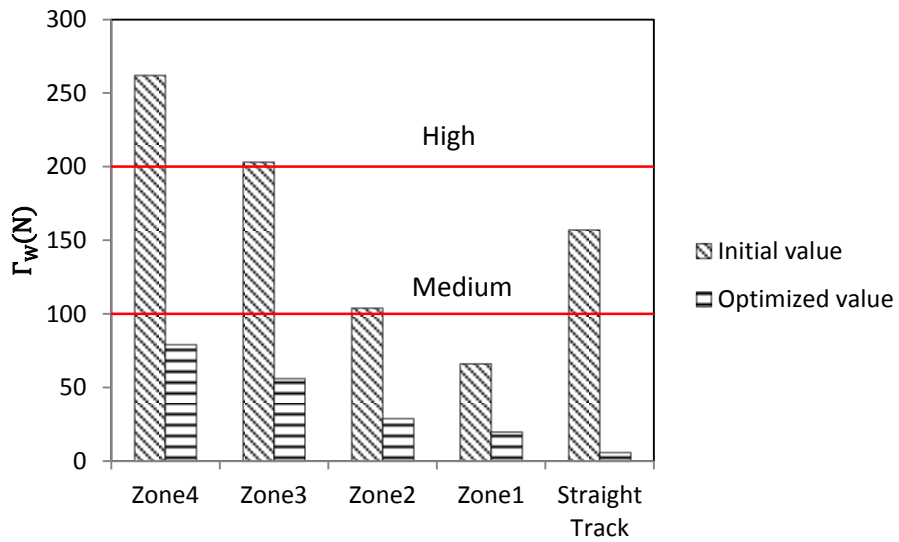


Figure 5.39 Initial and final value of wear objective function.

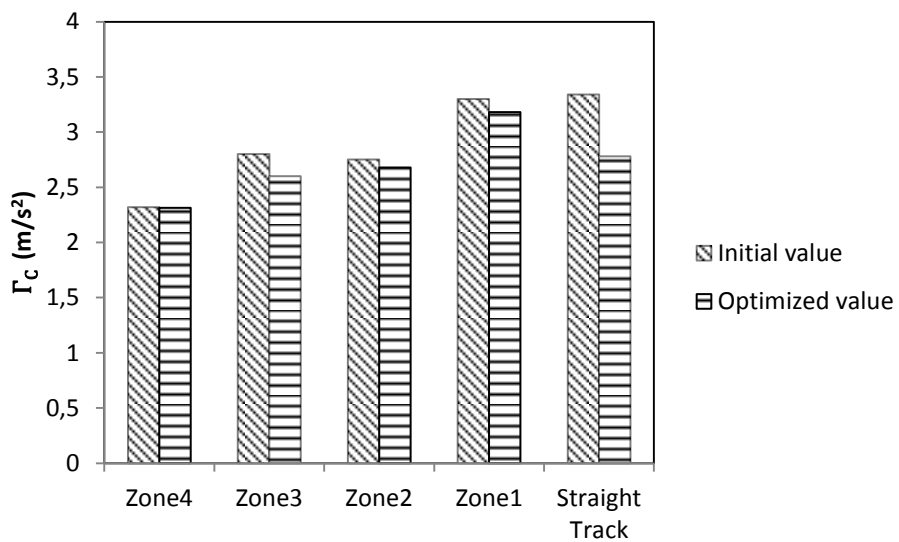


Figure 5.40 Initial and final value of comfort objective function.

6 Conclusion

In this chapter the work done during the development of this project is summarized. Moreover, final conclusions are obtained from the results achieved and several future work suggestions are given as continuations of the present work.

6.1 Summary

The first step towards the optimization of the primary passive suspension of a high-speed railway vehicle bogie is to have reliable engineering, mathematical and computational models. For this goal to be achieved, the Multi-Body simulation software SIMPACK v9.4 railway module is utilized to create a simple but reliable railway vehicle model as well as to perform the analysis of its dynamics behaviour. In this regard, a 50 degrees-of-freedom (DOFs) railway vehicle model created in SIMPACK composed of two bogie frames connected to four wheelsets and a car frame by means of the primary and the secondary passive suspension components, respectively is studied here. Both primary and secondary passive suspensions are introduced by parallel spring-dampers components in the longitudinal, lateral and vertical directions. To verify the model created, five general operational scenarios (with measured data as the track irregularities) have been used in SIMPACK simulations while the resulting values of the ride comfort, safety and wear objective functions have been measured and compared with the admissible values from different railway standards. In order to take advantage of Genetic Algorithm based optimization routines, the MATLAB SIMULINK-SIMPACT connection is considered.

The first set of optimization problems are focused on the optimization of the bogie primary suspension springs and dampers components with respect to the wheel-rail wear objective function while ride comfort and safety are taken as thresholds. The results obtained in this case have shown an important reduction in the wear rate for different operational scenarios, which lead to the wear rate values very close to or under the “Medium” level and have demonstrated the strong influence of the longitudinal and lateral primary passive stiffness on resulting wear. Moreover, the second optimization results provided a further reduction of the wear rate having thus values inside the “Low Wear” category in every scenario. In this way, the considerable influence of the primary damping coefficients in the wear rate reduction has been shown. As it has been stated in the previous chapter, the remaining objective functions are within the admissible limits in both optimizations.

In addition and using the results from the first set of optimization problems, a pair of bi-objective optimization problems with wheel-rail wear and ride comfort as objective functions have been considered through the variation of the bogie primary suspension springs and dampers characteristics as design parameters. The results obtained from the second set of optimizations can be considered as a refinement of the improvements achieved in the first one. In this way, the advances are small but can be seen in every scenario which can be concluded that the optimized values of the design parameters (bogie passive primary suspension stiffness and damping) are found for each operational scenario.

6.2 Future work

Taking advantage of the work done and the conclusions mentioned above, various work directions can be proposed as the future steps.

- In order to complete the optimization of the primary passive suspension of a high-speed railway vehicle, a multi-objective optimization problem is proposed taking into consideration the three objective functions under study in this project simultaneously, i.e. safety, ride comfort and wheel-rail wear.
- More advanced vehicle models, like using flexible elements instead of rigid bodies could be another point of interest.
- New optimization routines with the aim of reducing the computation time and the result accuracy.
- Application of different types of semi-active vibration controls using magneto-rheological dampers.
- The values of the optimized design parameters obtained in this work for each operational scenario can be used as a guideline to redesign the suspension system of an existing railway vehicle. Studying each particular case independently in terms of the most frequently scenario used and the range of the vehicle speed, a possible improvement of the wheel-rail wear can be achieved.
- Finally, the resulting optimized values of primary damping coefficients for the different cases can be used as a suggestion or initial point once implementing semi-active and/or fully active suspension instead of the passive one.

7 References

- Andersson, E., Berg, M., Stichel, S. (2007): *Rail Vehicle dynamics*. RAILWAY GROUP KTH, Centre for Research and Education in Railway Engineering.
- Banverket (1996): Tillåten hastighet m h t spårets geometriska form (In Swedish), BVF 586.41.
- Baumal, A.E., McPhee, J.J. and Calamai, P.H. (1996): Application of genetic algorithms to the design optimization of an active vehicle suspension system. *System Design Engineering, University of Waterloo, Waterloo, Ontario, Canada N2L 3G1*.
- CEN (Comité Européen de Normalisation) (1999): *Railway applications – Ride comfort for passengers – Measurement and evaluation*, ENV 12299.
- CEN (2005): *Railway applications – Testing for the acceptance of running characteristics of railway vehicles – Testing of running behaviour and stationary test*, EN-14363, Brussels, June.
- Cheng, Y.C., Lee, S.Y., Chen, H.H. (2009): *Modeling and nonlinear hunting stability analysis of high-speed railway vehicle moving on curved tracks*. Department of Mechanical Engineering, National Cheng Kung University, Tainan, Taiwan 701, ROC.
- Dukkipati, R. V., & Guntur, R. R. (1984): Design of a longitudinal railway vehicle suspension system to ensure the stability of a wheelset. *International Journal of Vehicle Design*, 5(5), 451–466.
- Fa, Y., Wu, W., (2006): Stability analysis of railway vehicles and its verification through field test data. *Journal of the Chinese Institute of Engineers*, Vol. 29, No. 3, pp. 493-505.
- Goldber, D.E. (1989): *Genetic Algorithms in Search, Optimization, and Machine Learning*. Addison-Wesley, Reading, Massachusetts.
- Goodall, R., (1999): Tilting trains and beyond – the future of active railway suspensions. *Computing & Control Engineering Journal*.
- Jalili, N., (2001): *Semi-Active Suspension Systems. The Mechanical Systems Design Handbook – Modeling, Measurement, and Control* (Chap. 12), ISBN 0-8493-8596-2, CRC Press.
- Johnsson, A., Berbyuk, V., Enelund, M. (2012). Pareto Optimisation of railway bogie suspension damping to enhance safety and comfort. *Vehicle System Dynamics: International Journal of Vehicle Mechanics and Mobility*, 50:9, 1379-1407, DOI:10.1080/00423114.2012.659846.
- López, A., (2004): *Railway, engineering and society* {Ferrocarril, ingeniería y sociedad}. Inaugural speech at Royal Academy of Engineering, ISBN 84-95662-23-X.
- Mei, T.X., Goodall, R.M., (2000): Modal controllers for active steering of railway vehicles with solid axle wheelsets, *Vehicle System Dynamics: International Journal of Vehicle Mechanics and Mobility*, 34:1, 25-41.

Mousavi, M., Berbyuk, V., (2013): Multiobjective optimization of a railway vehicle dampers using genetic algorithm. *Proceedings of the ASME2013 International Design Engineering Technical Conferences & Computers and Information in Engineering Conference, IDETC/CIE 2013, August 4-7, 2013, Portland, USA (Paper DETC 2013-12988)*

Orvnäs, A., (2011): *On Active Secondary Suspension in Rail Vehicles to Improve Ride Comfort*. PhD Thesis. Department of Aeronautical and Vehicle Engineering, KTH Engineering Sciences.

Pearce T.G. and Sherratt N.D (1991): *Prediction of Wheel Profile Wear*, Wear, Vol 144, Elsevier.

R.M. Goodall and T.X. Mei et all (2003): *Active stability control strategies for a high speed bogie*. Department of Electronic and Electrical Engineering, Loughborough University, Ashby Road, Loughborough, Leicestershire LE11 3TU, UK.

SIMPACK (2013): SIMPACK Documentation.

Sperling, E., (1941): *A method for evaluating the operating characteristics of railways* {Verfahren zur Beurteilung der Laufeigenschaften von Eisenbahnwesen}. Organ f.d. Fortschritte des Eisenbahnwesens, 12, pp. 176–187.

Sperling, E., and Betzhold, C., (1956): *Contribution to the evaluation of ride comfort in railway vehicles* {Beitrag zur Beurteilung des Fahrkomforts in Schienenfahrzeugen}. Glasers Annalen 80, pp. 314–320.

Suarez B., Mera J.M., Martinez M.L. and Chover J.A. (2012): Assessment of the influence of the elastic properties of rail vehicle suspension on safety, ride quality and track fatigue. *Vehicle System Dynamics: International Journal of Vehicle Mechanics and Mobility*.

Wang, D., Liao, W., (2003): *Ride quality improvement ability of semi-active, active and passive suspension systems for railway vehicles*. Smart Materials and Structures Laboratory. Department of Automation and Computer-Aided Engineering. The Chinese University of Hong Kong.